

Results of the First Interferometric Measurements of Undulator Radiation from Single Electrons

Giulio Stancari

Senior Scientist
Fermi National Accelerator Laboratory and
University of Chicago

- Motivation
- Experimental Methods
- Results

Contributors

Jonathan Jarvis (Fermilab): design, equipment, simulations

Ihar Lobach (UChicago, now Brookhaven): design, theory, equipment, controls

Sergei Nagaitsev (Fermilab and UChicago, now Brookhaven): supervision, design, equipment, funding

Aleksandr Romanov (Fermilab): design, beam operations, construction and controls, measurements

Alexander Shemyakin (Fermilab): design, construction and commissioning, measurements, data analysis, documentation

Giulio Stancari (Fermilab and UChicago): design, data acquisition system, measurements, data analysis, documentation

Alexander Valishev (Fermilab): supervision, funding

Thanks to **the whole IOTA/FAST group** for making the experiment possible, in particular

D. Broemmelsiek, D. Edstrom, D. MacLean, J. Ruan, J. Santucci and **T. Thompson**.

Special thanks to **Zhirong Huang** (SLAC) for his support and for providing the undulator.

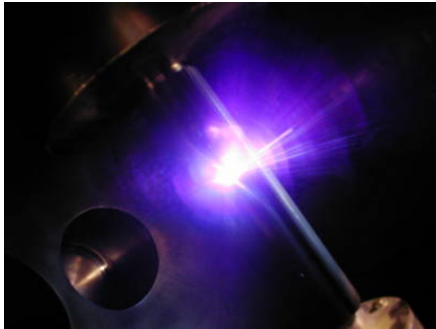
Work supported in part by a **Fermilab Laboratory-Directed Research and Development (LDRD) grant**, “Quantum Effects in Undulator Radiation,” FNAL-LDRD-2019-025 and by the **UChicago Consortium for Advanced Science and Engineering (CASE)**

Motivation

Can we **directly observe the classical or quantum properties of radiation from single electrons** and electron bunches?

Are there new ways to **generate quantum states of light**?

Are there novel **applications** of the experimental techniques **of quantum optics in accelerator physics** and **beam diagnostics**?



Mandel and Wolf, *Optical Coherence and Quantum Optics* (Cambridge, 1995)

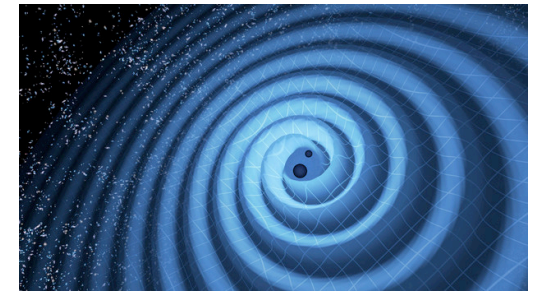
Grishaev et al., *Sov. Phys. JETP* **32**, 16 (1971); **36**, 870 (1973)

Pinayev et al., *NIM A* **341**, 17 (1994)

Nagaitsev et al., *FERMILAB-TM-2804-AD* (2022)

Stancari et al., *IPAC* (2024)

[Connection with **gravitation**? As quantum sensors approach graviton sensitivity, **experimental tests of the coherent-state description of radiation fields** may in the future help to understand the interplay between quantum physics and gravity]



Tobar et al., *Nat. Commun.* **15**, 7229 (2024)

Manikandan and Wilczek, *Phys. Rev. A* **111**, 033705 (2025)



Quantum States of Radiation

Physical system

classical electromagnetic wave

dipole antenna, laser, ...

thermal, “chaotic” source

light bulb, black body, star, ...

quantized radiation from
single atom, parametric down-
conversion, quantum dot, ...

Corresponding quantum state

Glauber *coherent state*

$$\hat{a} |\alpha\rangle = \alpha |\alpha\rangle$$

$$|\alpha\rangle = e^{-|\alpha|^2/2} \sum_{n=0}^{\infty} \frac{\alpha^n}{\sqrt{n!}} |n\rangle$$

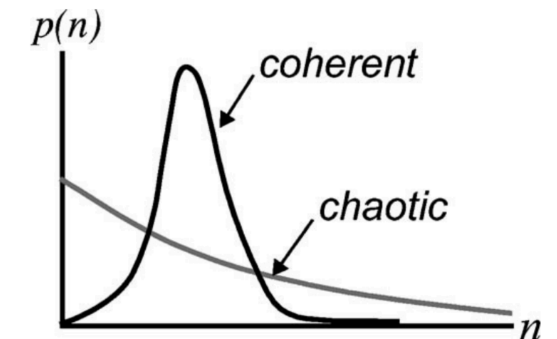
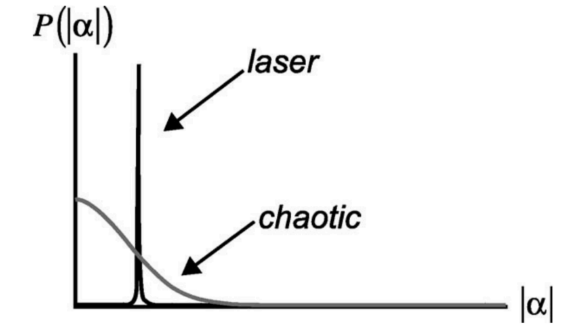
incoherent mixture

(density matrix)

Fock *number state*

$$\hat{n} |1\rangle = 1 |1\rangle$$

$$\hat{n} |2\rangle = 2 |2\rangle$$



Quantum states can be identified experimentally by recording **photoncount statistics**:

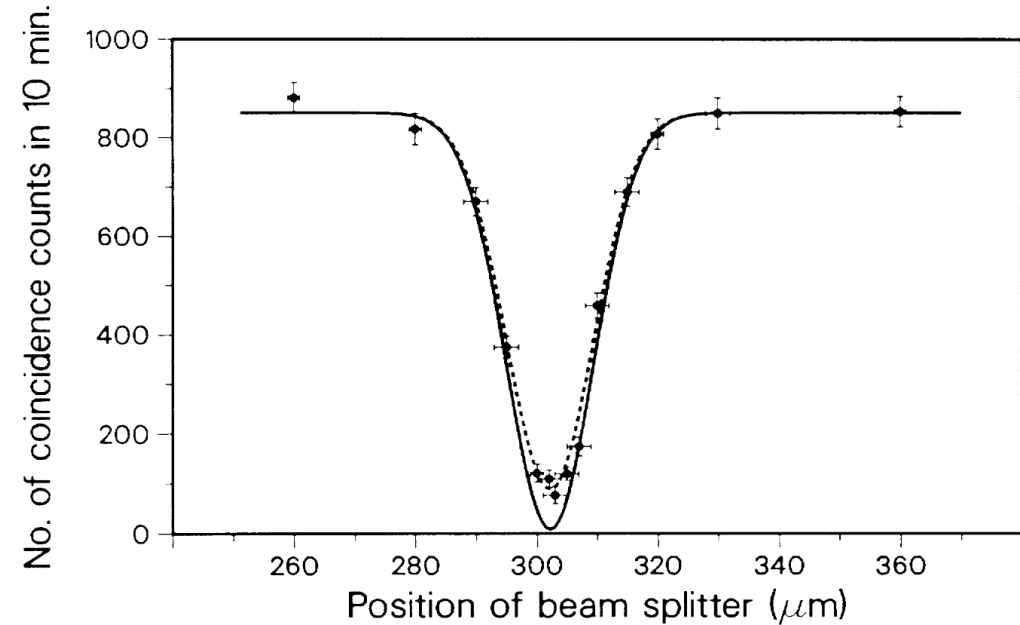
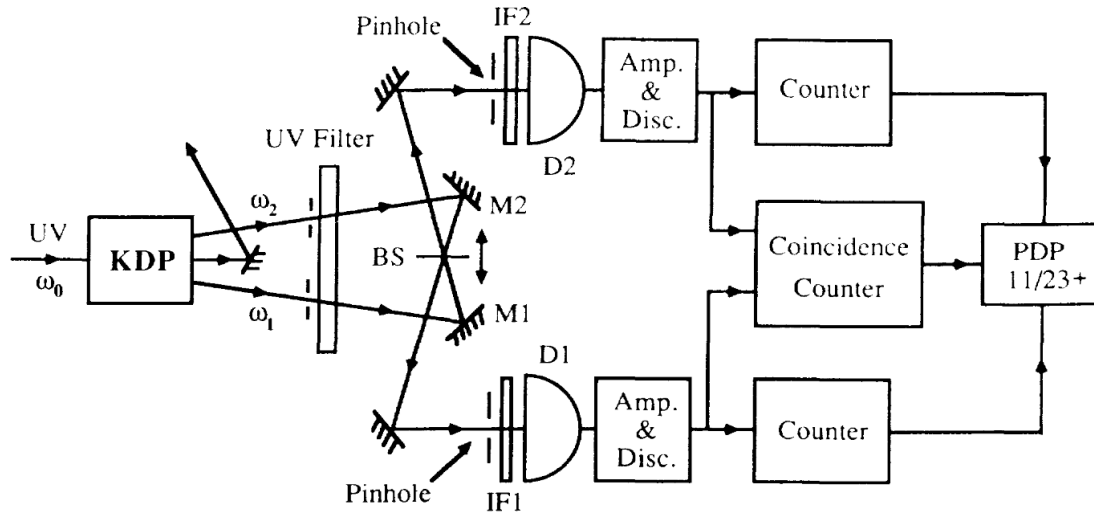
intensity fluctuations, arrival time distributions, coincidences vs. delay

Glauber, Rev. Mod. Phys. **78**, 1267 (2006)

Mandel and Wolf, Optical Coherence and Quantum Optics (Cambridge, 1995)

The Hong-Ou-Mandel (HOM) Effect

UV laser light split into 2 longer wavelengths in nonlinear crystal



Within coherence time, radiation in a 2-photon state is observed in the same detector

Coincidences are suppressed

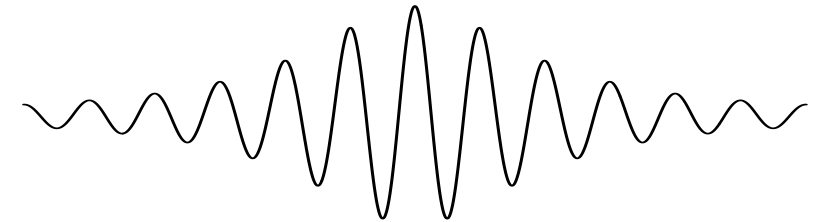
Hong, Ou and Mandel, PRL **59**, 2044 (1987)



Note on the Usage of “Coherence”

“Coherence” and “coherent” have several meanings in physics. In this talk:

temporal coherence is characterized by **coherence length** L_c or **coherence time** L_c / c interval over which the light wave at a certain location has a defined phase inversely proportional to the spectral width for quasi-monochromatic radiation



coherent state

quantum state of radiation

eigenstate of the field amplitude (annihilation) operator

a superposition of number states

describes classical waves

$$\hat{a} |\alpha\rangle = \alpha |\alpha\rangle$$

$$|\alpha\rangle = e^{-|\alpha|^2/2} \sum_{n=0}^{\infty} \frac{\alpha^n}{\sqrt{n!}} |n\rangle$$



Properties of Undulator Radiation: Research at IOTA

Fluctuations in undulator radiation (FUR experiment)

How do fluctuations scale with intensity (sub/super-Poissonian)?
Can fluctuations be used for beam diagnostics?

Lobach et al., PRAB **23**, 090703 (2020)
Lobach et al., PRAB **24**, 040701 (2021)
Lobach et al., PRL **126**, 134802 (2021)
Lobach, PhD Thesis (2021)

Photocount statistics of radiation with single or few electrons (URSSE experiment)

What can we learn about the quantum state of radiation from photocount statistics?
What properties of the beam can we measure?

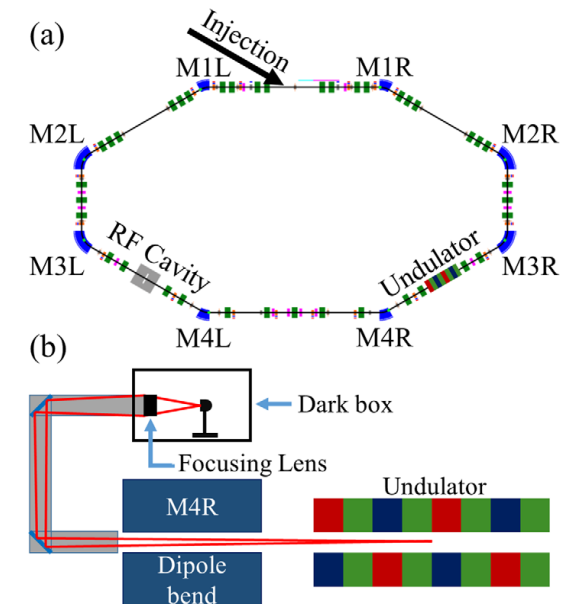
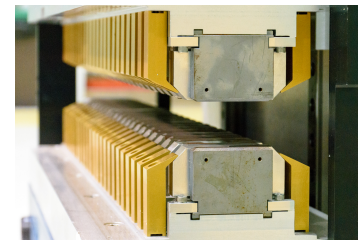
Lobach, PhD Thesis (2021)
Lobach et al., JINST **17**, P02014 (2022)

Interferometry of single-electron radiation (CLARA experiment)

What is the temporal coherence?
Is radiation in a classical or quantum state?

← this presentation

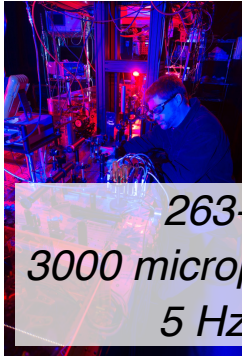
Nagaitsev et al., FERMILAB-TM-2804-AD (2022)
Stancari et al., IPAC 2024





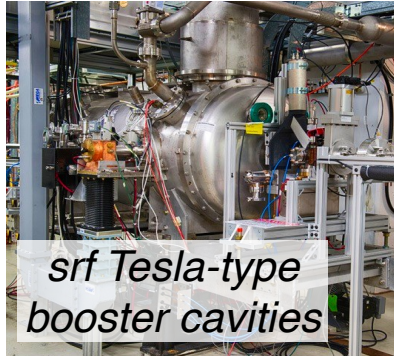
Overview of the IOTA/FAST Facility at Fermilab

Photoinjector



263-nm laser
3000 micropulses @ 3 MHz
5 Hz rep. rate

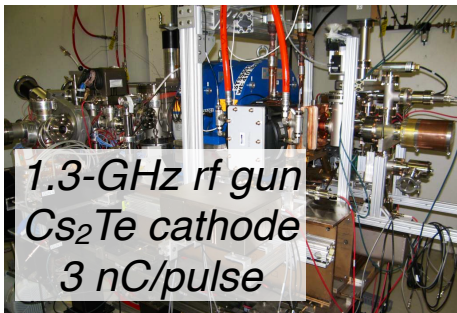
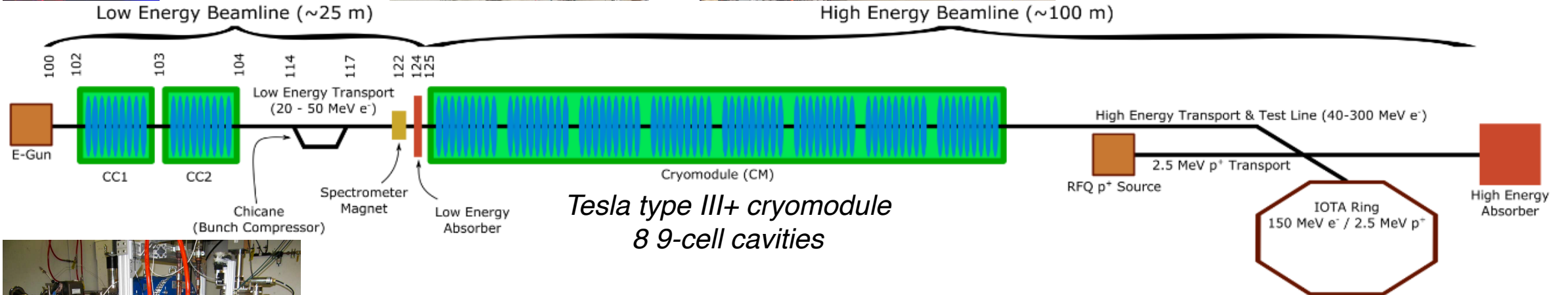
Superconducting Linac



srf Tesla-type
booster cavities

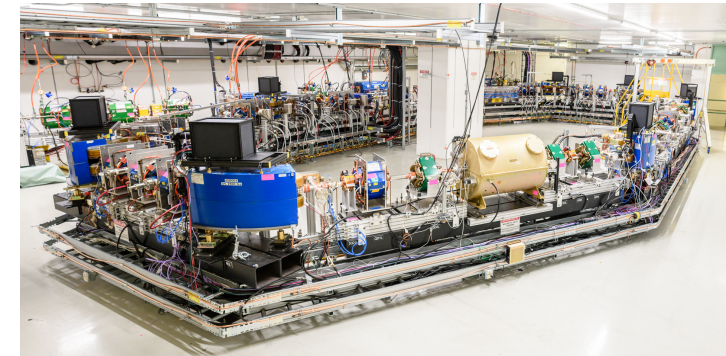


High Energy Beamline (~100 m)



1.3-GHz rf gun
Cs₂Te cathode
3 nC/pulse

IOTA Storage Ring



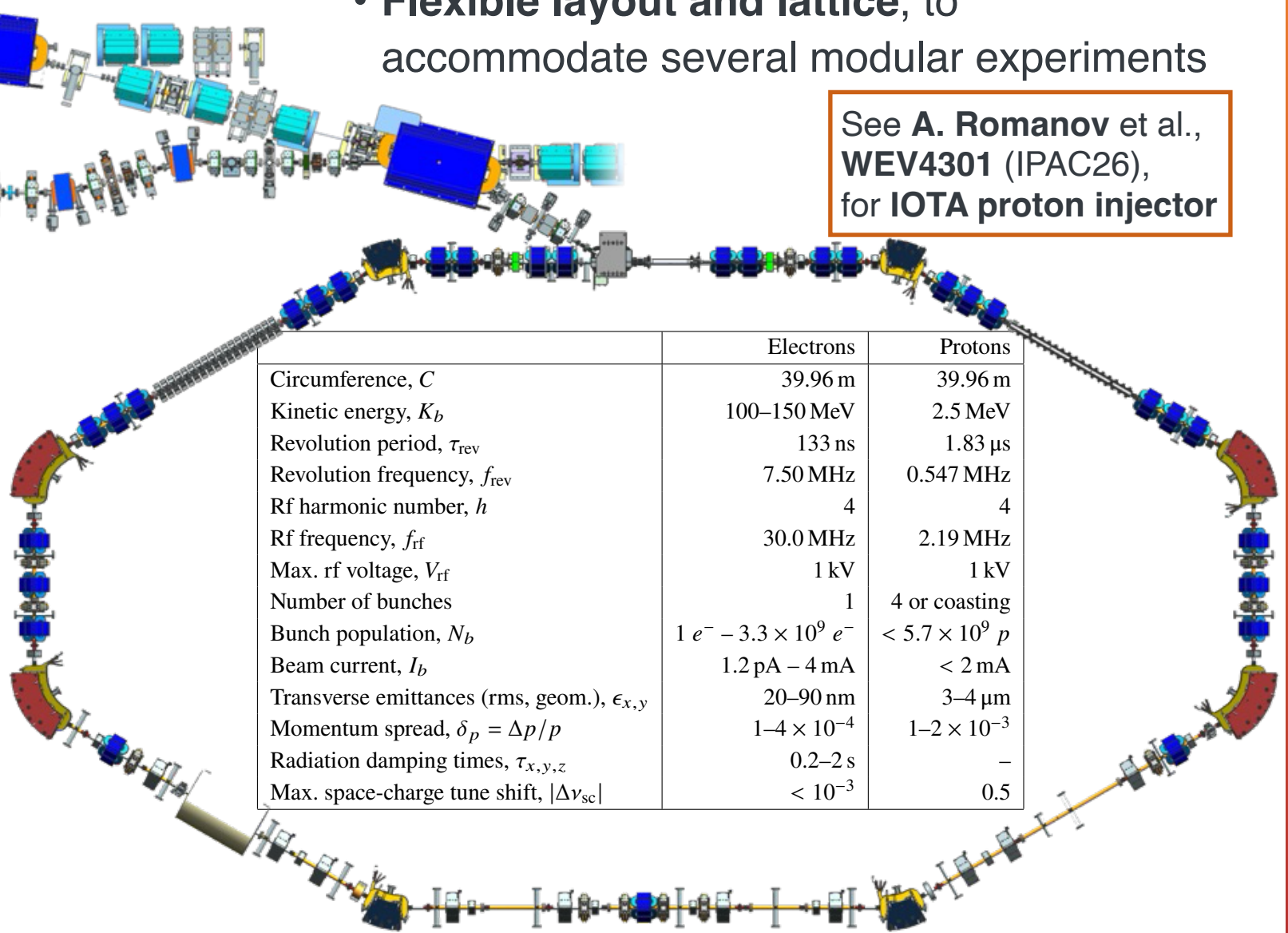
Antipov et al., JINST **12**, T03002 (2017)
Broemmelsiek et al., New J. Phys. **20**, 113018 (2018)

The IOTA Storage Ring

- **Dedicated to beam physics research**
- **Flexible layout and lattice**, to accommodate several modular experiments

See **A. Romanov et al., WEV4301 (IPAC26), for IOTA proton injector**

- Can store
 - **electrons** up to 150 MeV
 - fast synchrotron-radiation damping, nonlinear “single-particle” dynamics
 - **protons** at 2.5 MeV
 - studies with strong space charge
- Accurate beam optics
- Large **aperture** (50 mm)
- Advanced **instrumentation**



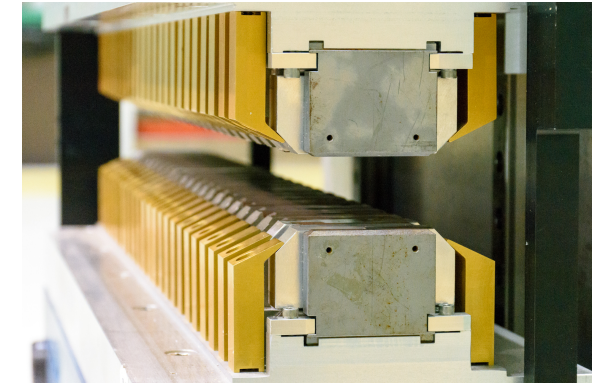
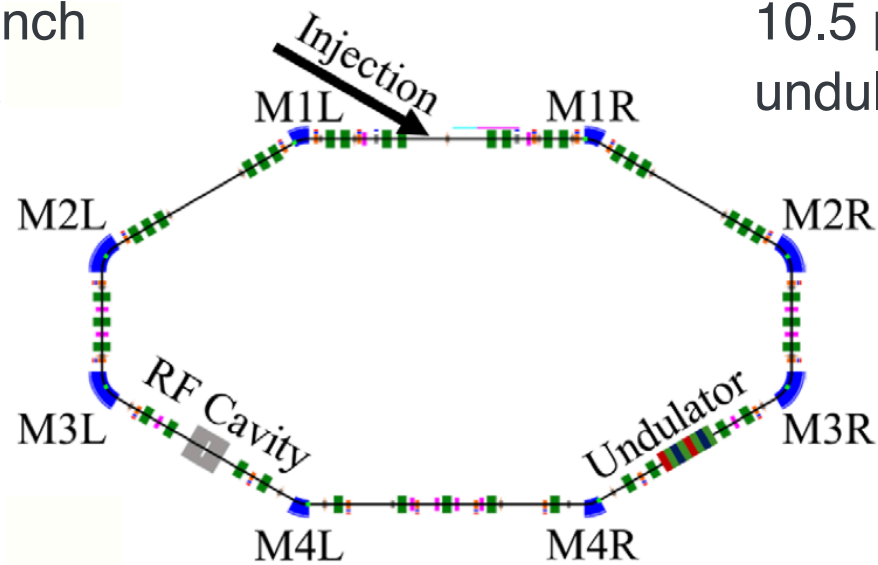
	Electrons	Protons
Circumference, C	39.96 m	39.96 m
Kinetic energy, K_b	100–150 MeV	2.5 MeV
Revolution period, τ_{rev}	133 ns	1.83 μs
Revolution frequency, f_{rev}	7.50 MHz	0.547 MHz
Rf harmonic number, h	4	4
Rf frequency, f_{rf}	30.0 MHz	2.19 MHz
Max. rf voltage, V_{rf}	1 kV	1 kV
Number of bunches	1	4 or coasting
Bunch population, N_b	$1 e^- - 3.3 \times 10^9 e^-$	$< 5.7 \times 10^9 p$
Beam current, I_b	1.2 pA – 4 mA	< 2 mA
Transverse emittances (rms, geom.), $\epsilon_{x,y}$	20–90 nm	3–4 μm
Momentum spread, $\delta_p = \Delta p/p$	$1-4 \times 10^{-4}$	$1-2 \times 10^{-3}$
Radiation damping times, $\tau_{x,y,z}$	0.2–2 s	–
Max. space-charge tune shift, $ \Delta\nu_{\text{sc}} $	$< 10^{-3}$	0.5



Experimental Apparatus

Electrons in IOTA at 150 MeV
 10^9 — 1 electrons per bunch
 Revolution period 133 ns
 Bunch length 0.7 ns

SLAC undulator (NLCTA-Echo 7)
 10.5 periods of length 55 mm each
 undulator parameter $K_u = 1.06$

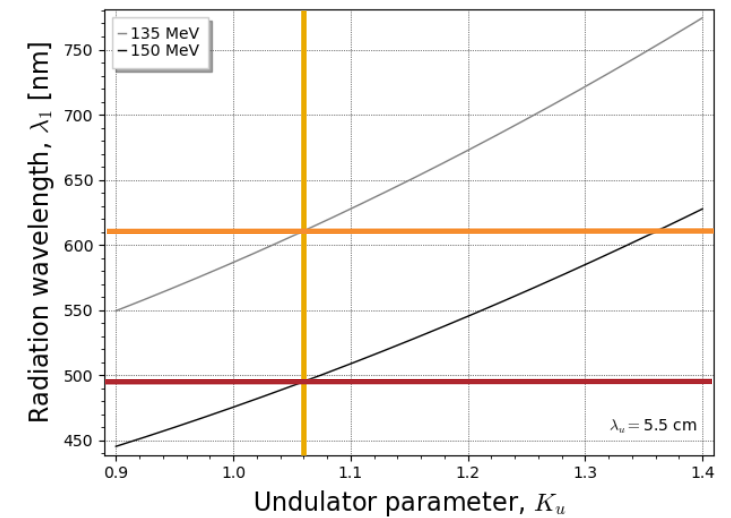
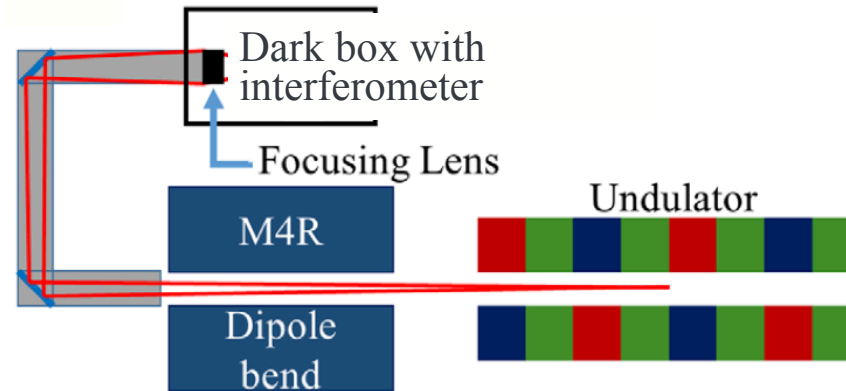
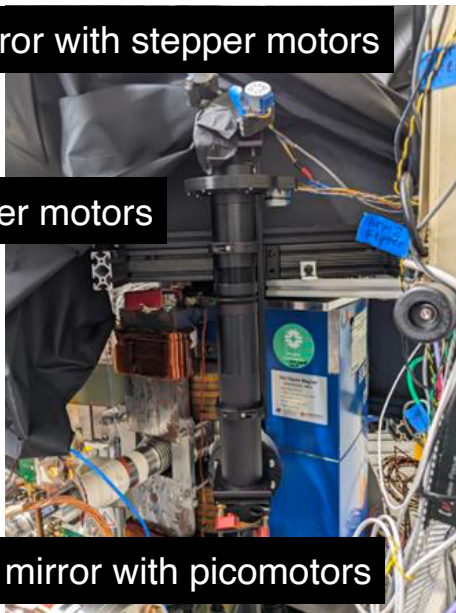


Light collection

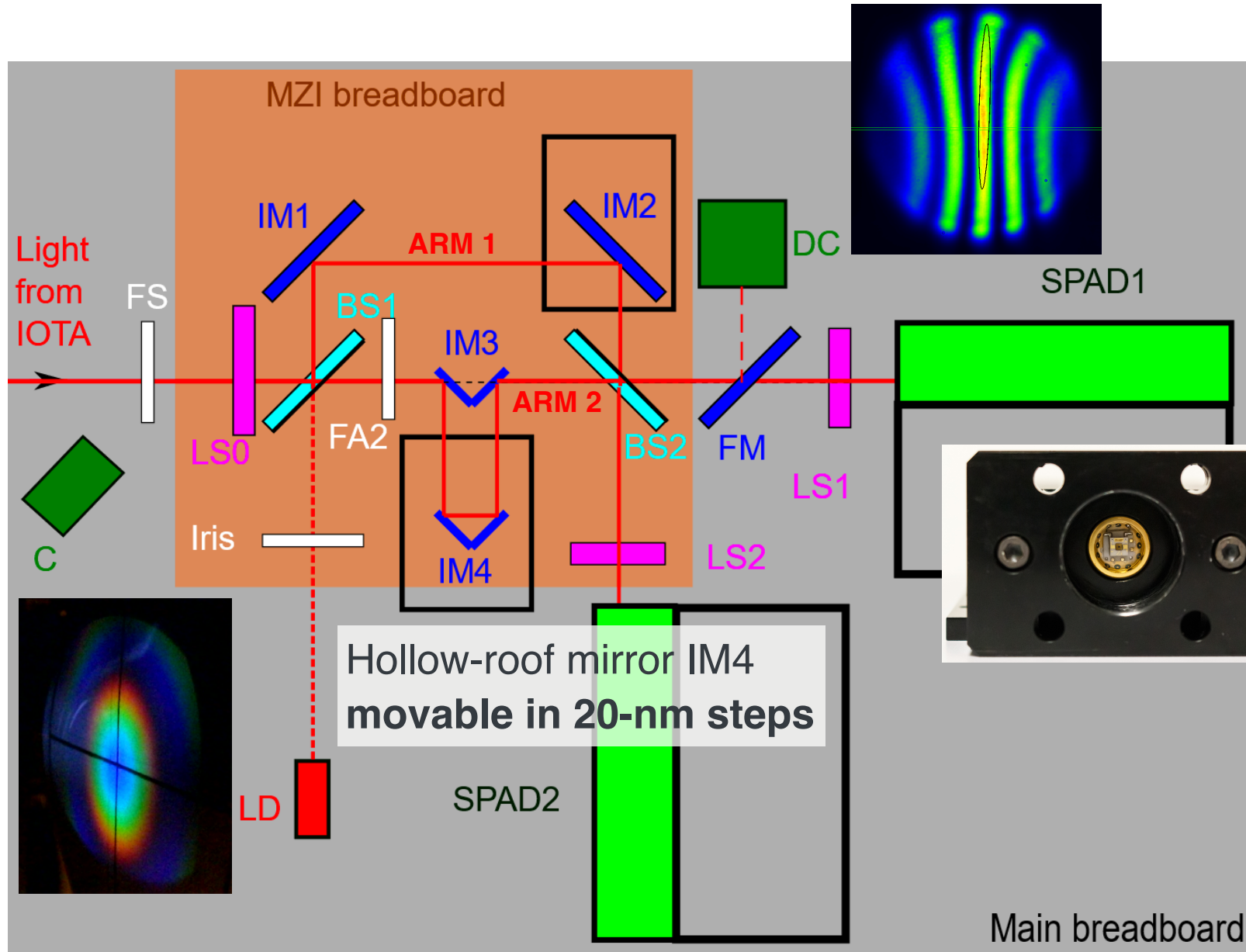
Top mirror with stepper motors

Iris with stepper motors

Bottom mirror with picomotors



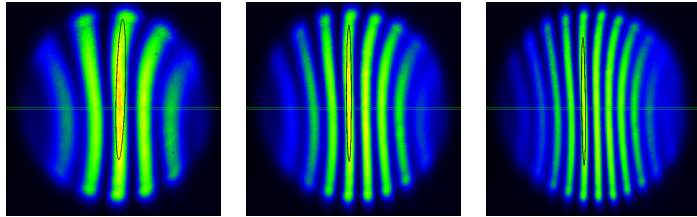
The Mach-Zehnder Interferometer (MZI)



- BS1, 2 — Beam splitters
- C — Webcam
- DC — Digital camera
- FA2 — Arm-2 flipping screen
- FM — Flipping mirror
- FS — Flipping screen
- IM1, 2 — Arm-1 mirrors
- IM3 — Arm-2 right-angle mirror
- IM4 — Arm-2 hollow-roof mirror
- Iris — Laser collimator
- LD — Laser diode
- LS0 — Entrance lens
- LS1, 2 — Detector lenses
- SPAD1, 2 — Photodetectors

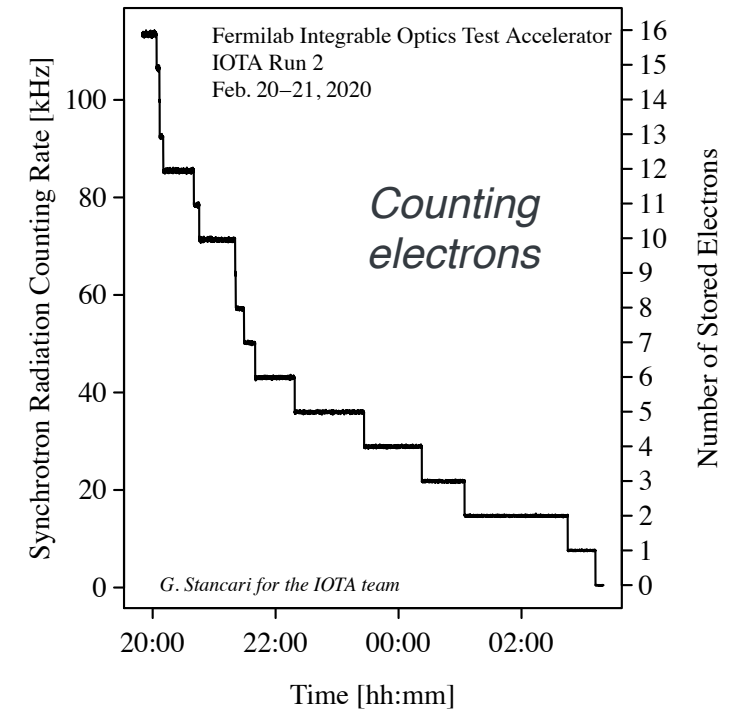
Experimental Procedure

- Inject full-intensity beam (~ 1 mA)
- Move beam from injection to central orbit
- Align periscope to center of iris and camera
- Establish interference conditions
- Measure alignment and fringe visibility with camera



Undulator radiation on screen FS with wide and narrow iris

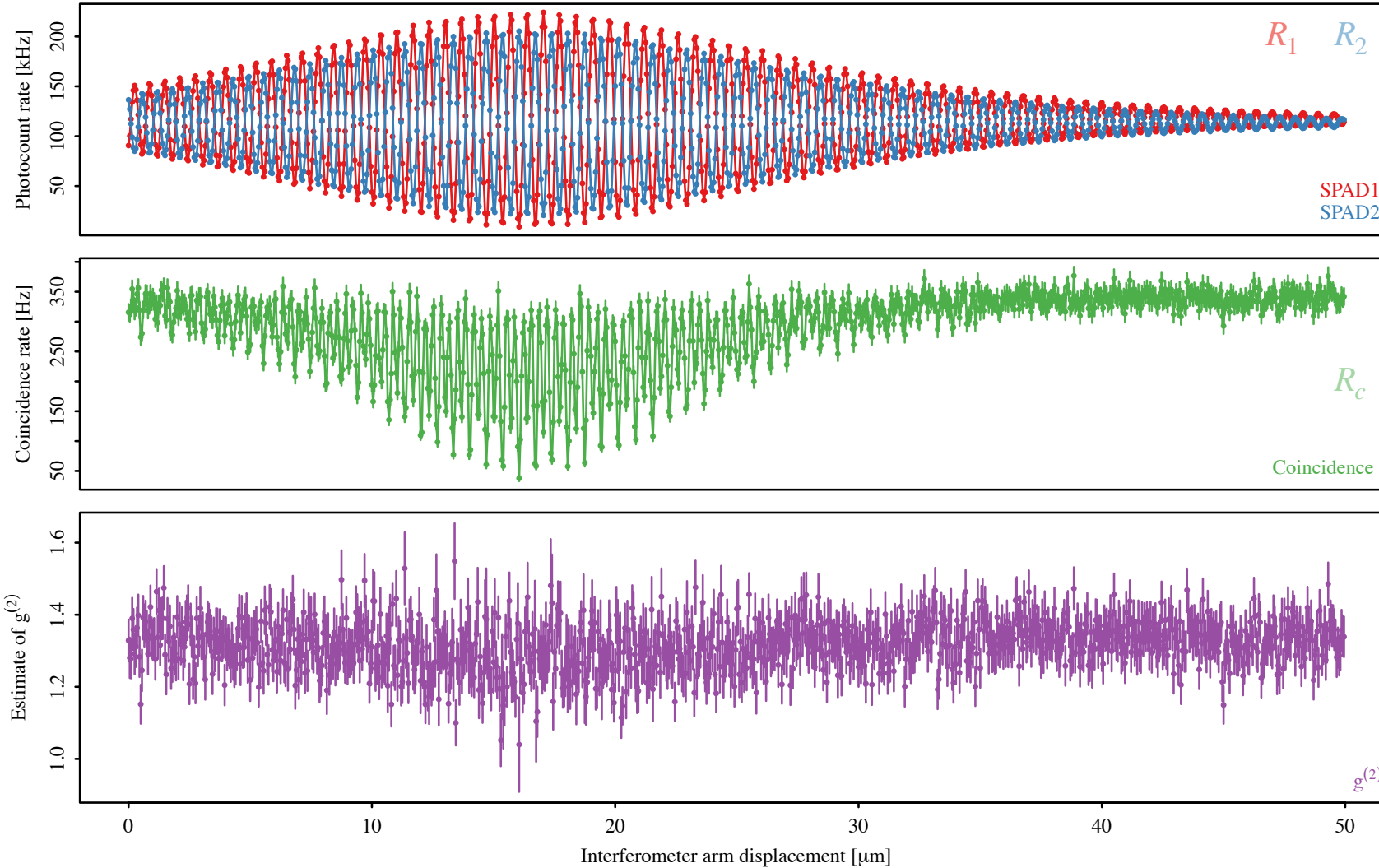
- Scrape beam to ~ 100 s of electrons by reducing rf voltage
- Check beam intensity with camera and photomultipliers
- Turn on SPADs
- Align SPADs in 3 directions
- Collect SPAD rates and time-tagged photocounts under various conditions: number of electrons, MZI arm delay, iris opening





Delay Scans with Laser Diode as Light Source

CLARA MZI stage scan
Diode 10 uA 2023-01-18 14:36:31.88



Diode far below lasing threshold
coherence length $\sim 10 \mu\text{m}$
($> \text{cm}$ when lasing)

Normalized
coincidence rate

$$r_c \equiv \frac{R_c}{R_1 \cdot R_2 \cdot t_w} \simeq g^{(2)}$$

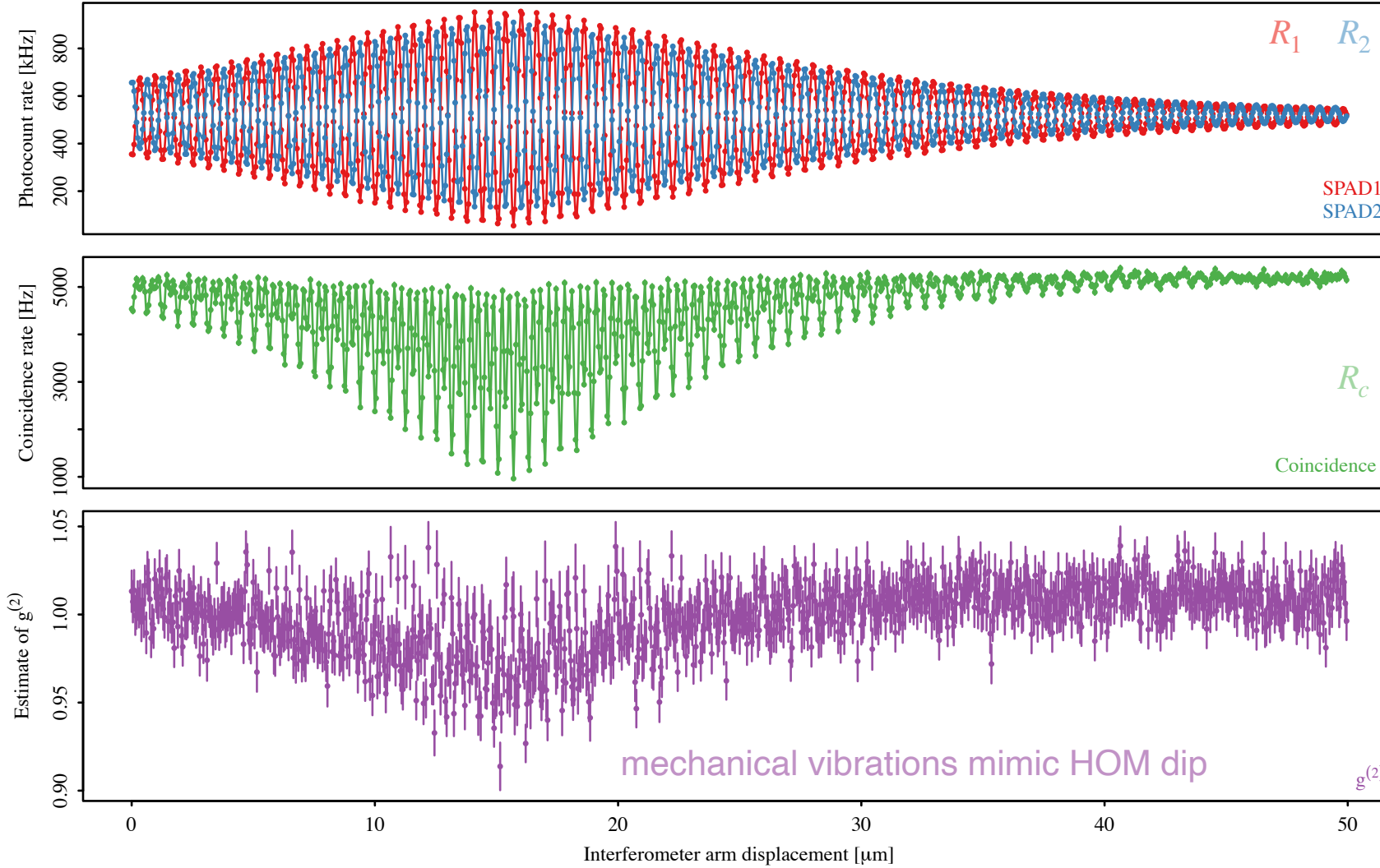
$$r_c > 1$$

indicates deviations from a pure coherent state:
thermal light, spontaneous emission



Delay Scans with Laser Diode as Light Source

CLARA MZI stage scan
Diode 22 mA 2023-01-19 16:35:53.25



Diode approaches lasing
coherence length still ~ 10 μm

Normalized
coincidence rate

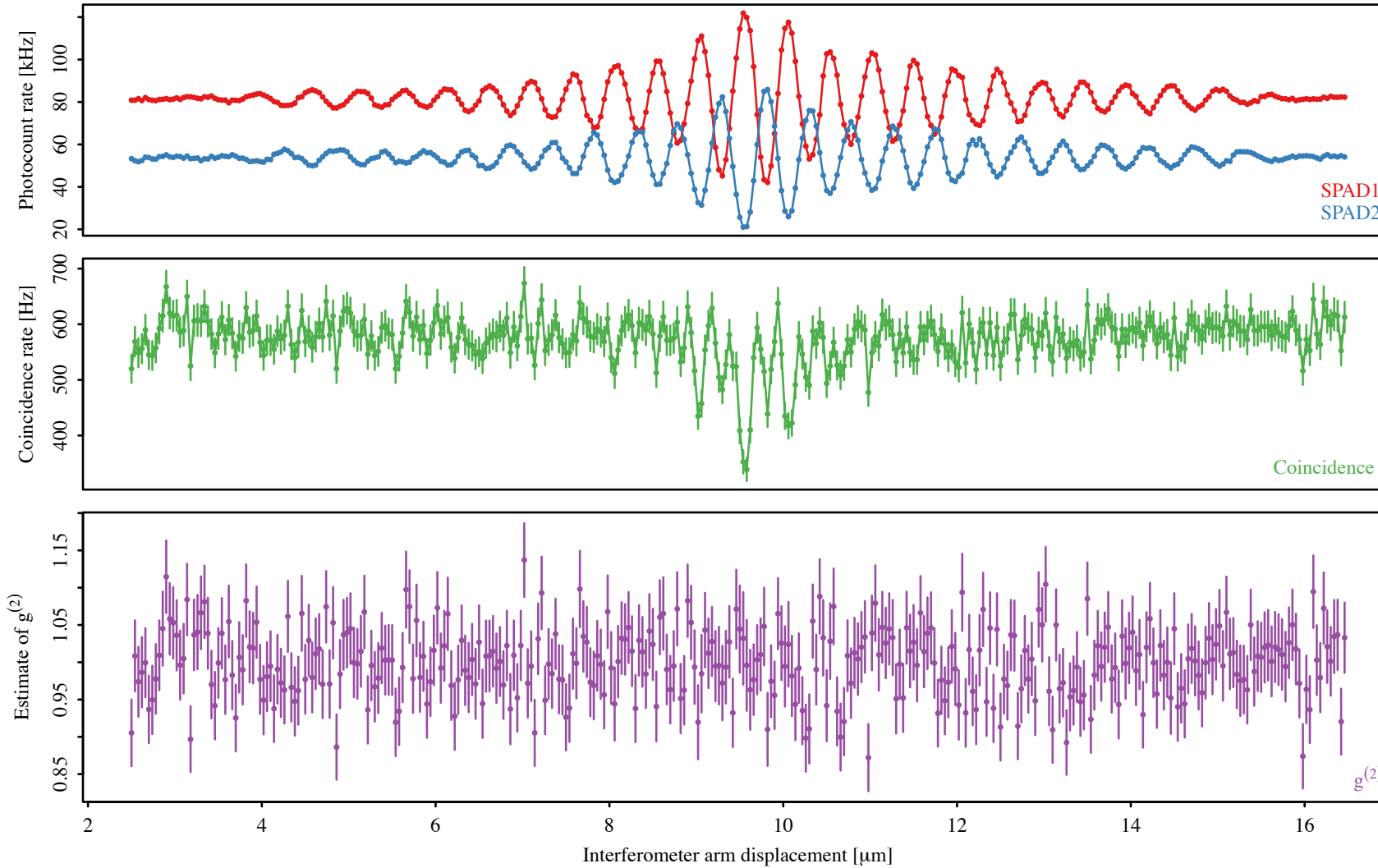
$$r_c \equiv \frac{R_c}{R_1 \cdot R_2 \cdot t_w} \simeq g^{(2)}$$

$r_c \simeq 1$ indicates light approaching a coherent state



Delay Scan with 13 Electrons in IOTA

CLARA MZI stage scan
13e full closed 2023-05-24 14:59:34.5



Coherence length $\sim 1 \mu\text{m}$

Normalized coincidence rate

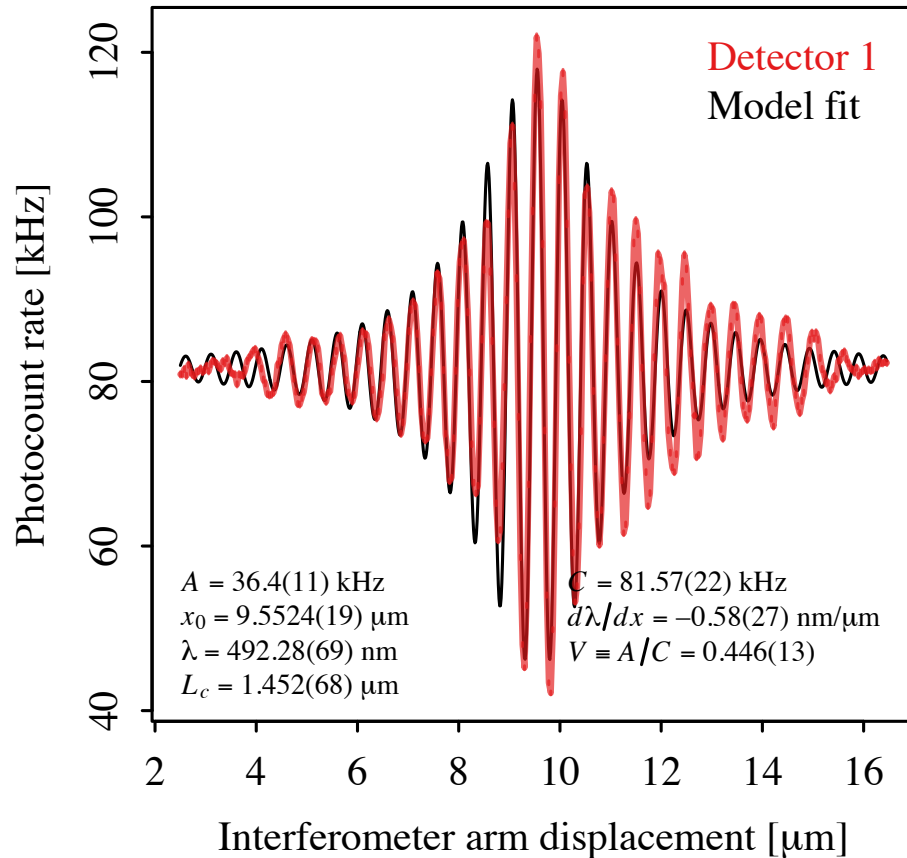
$$r_c \equiv \frac{R_c}{R_1 \cdot R_2 \cdot t_w} \simeq g^{(2)}$$

$r_c = 1$ indicates light in a coherent state



Interferogram Analysis to Estimate Coherence Length

13e full closed 2023-05-24 14:59:34.5



Model: sinusoid with Lorentzian envelope

$$R(x) = A \frac{\cos [2\pi(x - x_0)/\lambda']}{1 + [(x - x_0)/L_c]^2} + C$$

coherence length

$$\lambda' = \lambda + \left(\frac{d\lambda}{dx} \right) (x - x_0)$$

wavelength allowed to slightly vary with displacement to account for non-monochromatic spectrum and stage calibration uncertainty

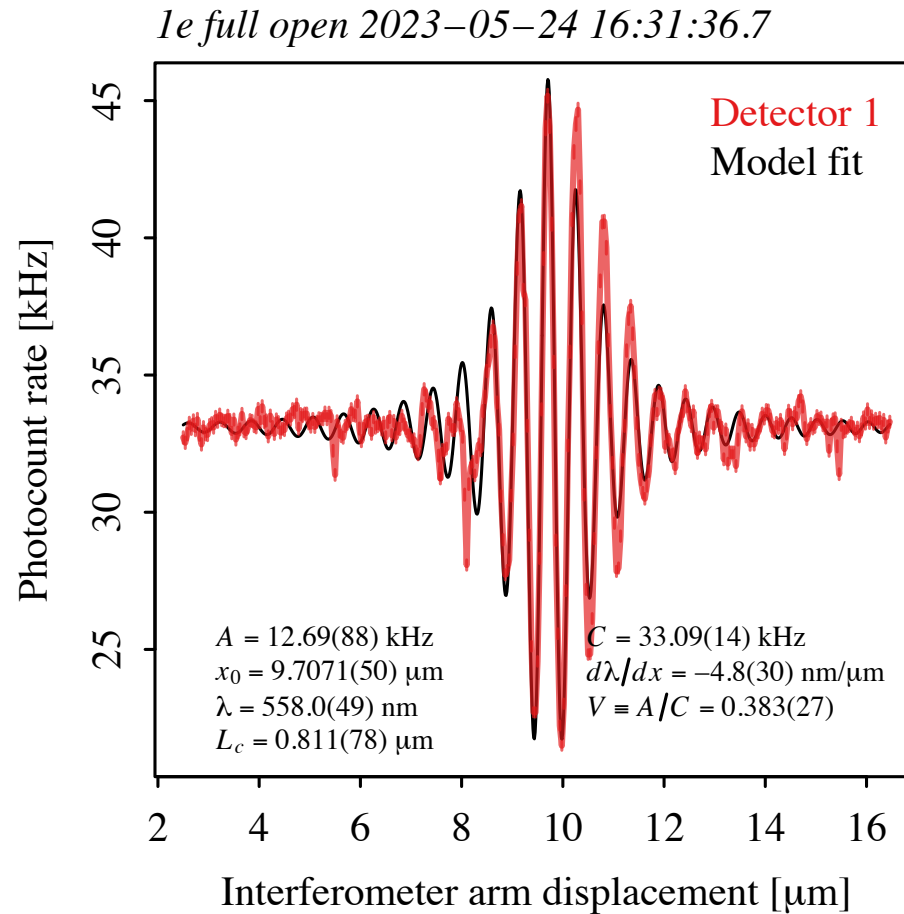
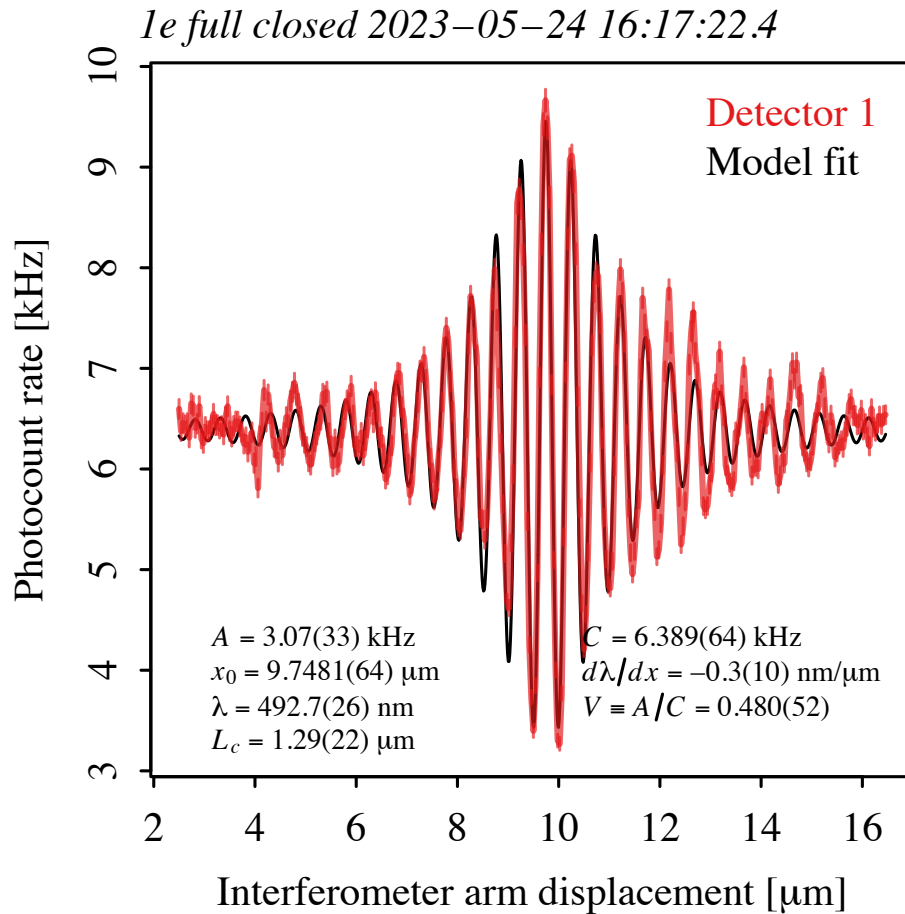
In general, envelope shape depends on spectrum of radiation



Interferograms of Single Electron!

narrow iris aperture

wide iris aperture

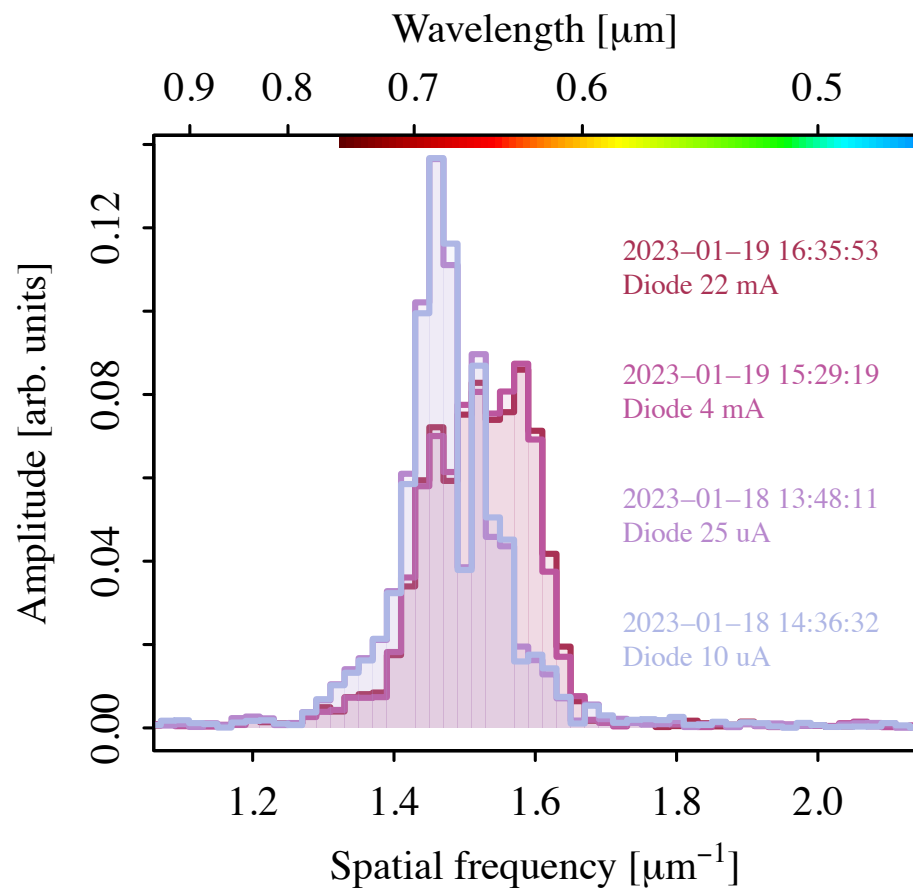


Changes in coherence length can be observed directly

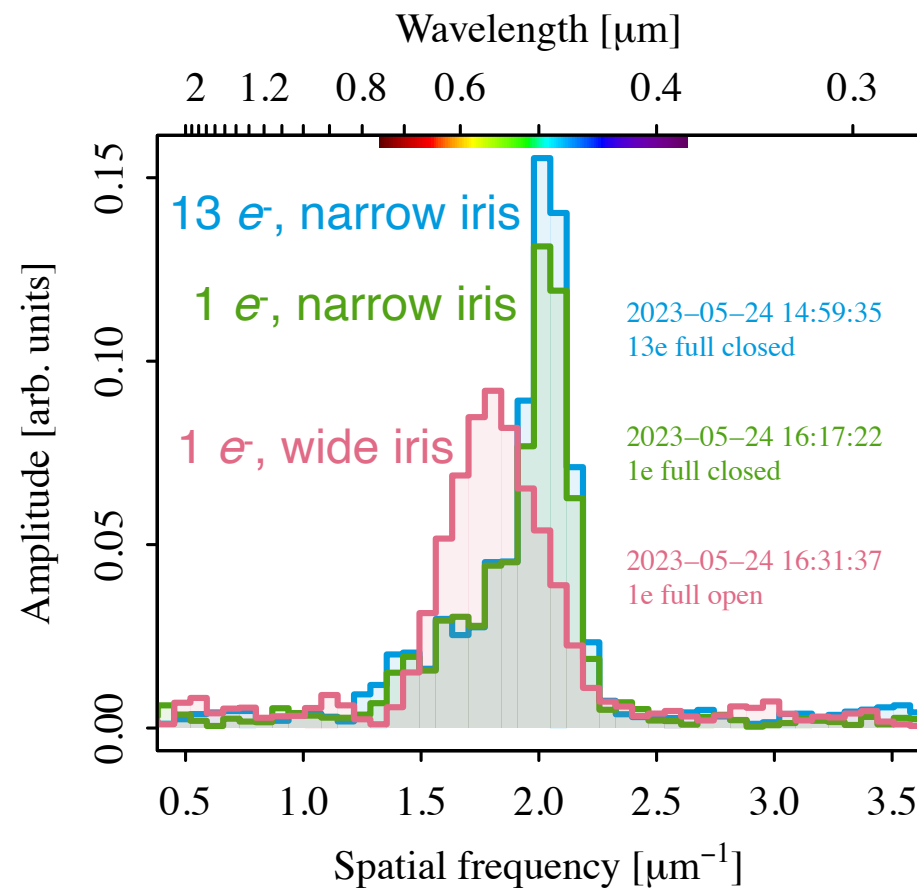


Interferogram Spectra

laser diode vs. current, below lasing threshold



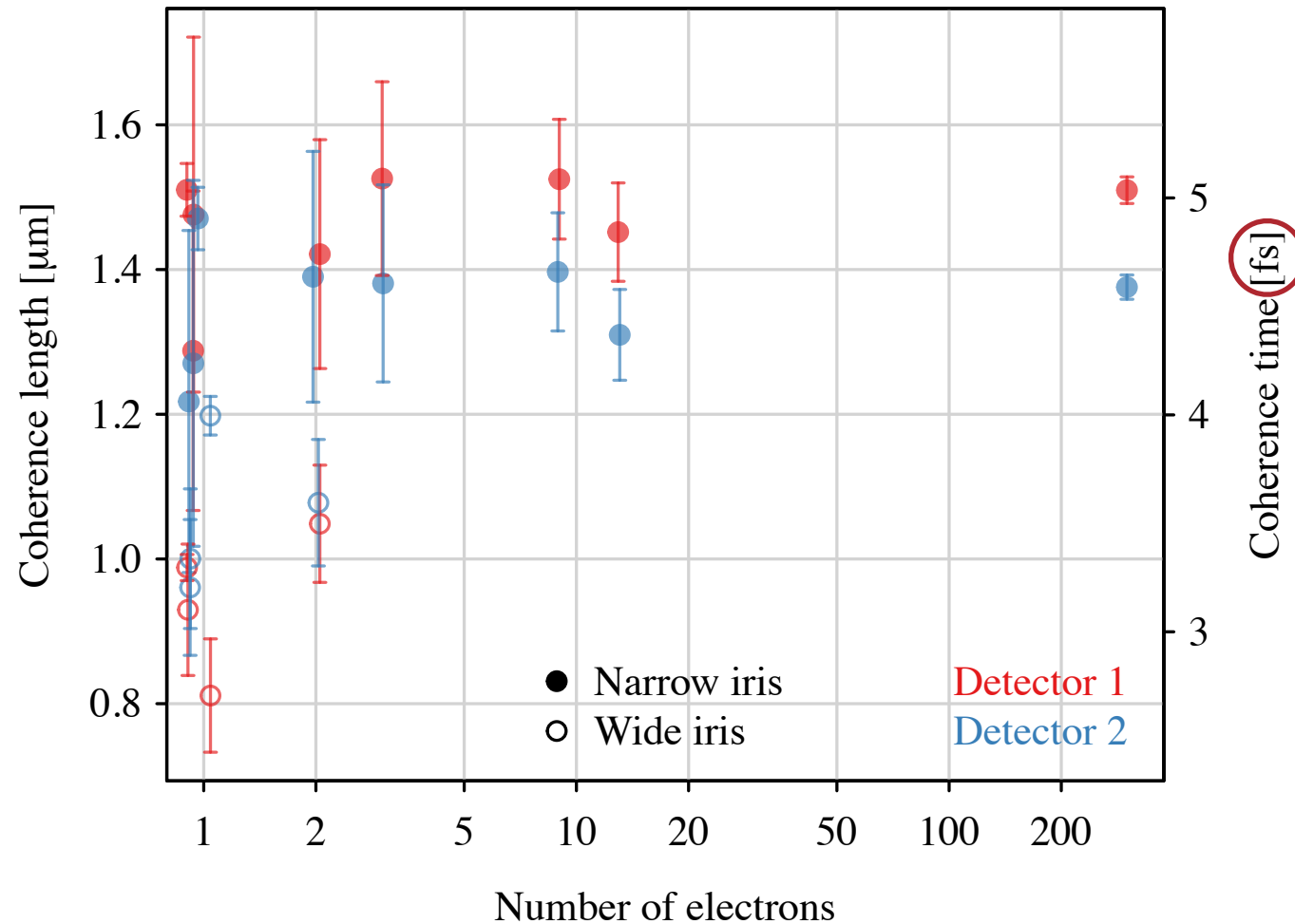
electron beam in undulator



The spectrum of undulator radiation can be observed directly, even for 1 electron



Coherence Length vs. Number of Electrons and Iris Size



**Femtosecond sensitivity
on coherence time of
emitted photons**

Coherence length is consistent for different numbers of electrons: 1, 2, 3, 9, 13, 300
The effect of iris aperture is clearly visible



Outlook: Quantum Optics in Beam Physics

Quantum-optical methods for beam diagnostics

Hanbury Brown and Twiss (HBT) intensity interferometry has been used to measure the size of stars and the luminosity distribution of celestial objects.

Are there other techniques in quantum optics that can be used as sensitive beam diagnostic monitors?

Generating quantum states of light

Synchrotron-light sources focus on intensity, spectrum, polarization, time structure.

Are there new ways to generate quantum states of radiation in storage rings?

What types of experiments would benefit from radiation in a specific number state (single photon, two photons, etc.)?

Conclusions

Directly observed temporal coherence of undulator radiation from single electrons at the femtosecond scale!

Estimated spectrum of radiation down to single electrons

Compared laser diode with undulator radiation. **Data confirm that undulator radiation of individual electrons is in a pure coherent state.** Full analysis of photocount statistics in progress.

Fascinating fundamental physics and potential novel applications for beam diagnostics

IOTA/FAST facility at Fermilab dedicated to beam physics research and education for the community: Ideas and collaborations always welcome





IOTA/FAST Collaboration Meeting, March 2024



Fermilab

Fermi *FORWARD*



U.S. DEPARTMENT
of ENERGY



Backup Slides



Theories of Light

Classical electromagnetism

Light as a field wave

Explains refraction, interference, diffraction, dispersion, synchrotron radiation, ...

Semi-classical approach

Classical light, quantum matter

Explains most phenomena in atomic and molecular physics: spectroscopy, stimulated emission, lasers, Zeeman effect, magneto-optical traps, ...

Quantum optics

The electromagnetic field is quantized with boson properties

Explains spontaneous emission, Lamb shift, Hong-Ou-Mandel effect, ...

Ambiguity of the word “photon:”

- photocounts
- energy quanta
- excitations of the field
- fuzzy balls of light
- ...

Mandel and Wolf, *Optical Coherence and Quantum Optics* (Cambridge, 1995)

Loudon, *The Quantum Theory of Light* (Oxford, 2000)

Grynberg, Aspect and Fabre, *Introduction to Quantum Optics* (Cambridge, 2010)

Bachor and Ralph, *A Guide to Experiments in Quantum Optics* (Wiley, 2019)



How Can One Measure the Quantum State of Radiation?

Main observables

Photocount statistics: intensity fluctuations, arrival time distributions

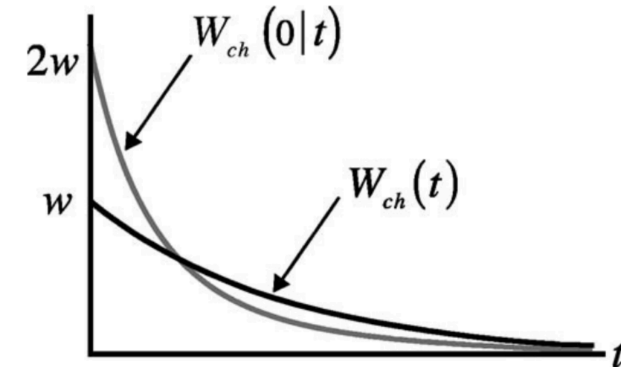
coherent state

$$W_{\text{coh}}(t) = W_{\text{coh}}(0|t) = we^{-wt}$$

chaotic state

$$W_{\text{ch}}(t) = \frac{w}{(1 + wt)^2}$$

$$W_{\text{ch}}(0|t) = \frac{2w}{(1 + wt)^3}$$

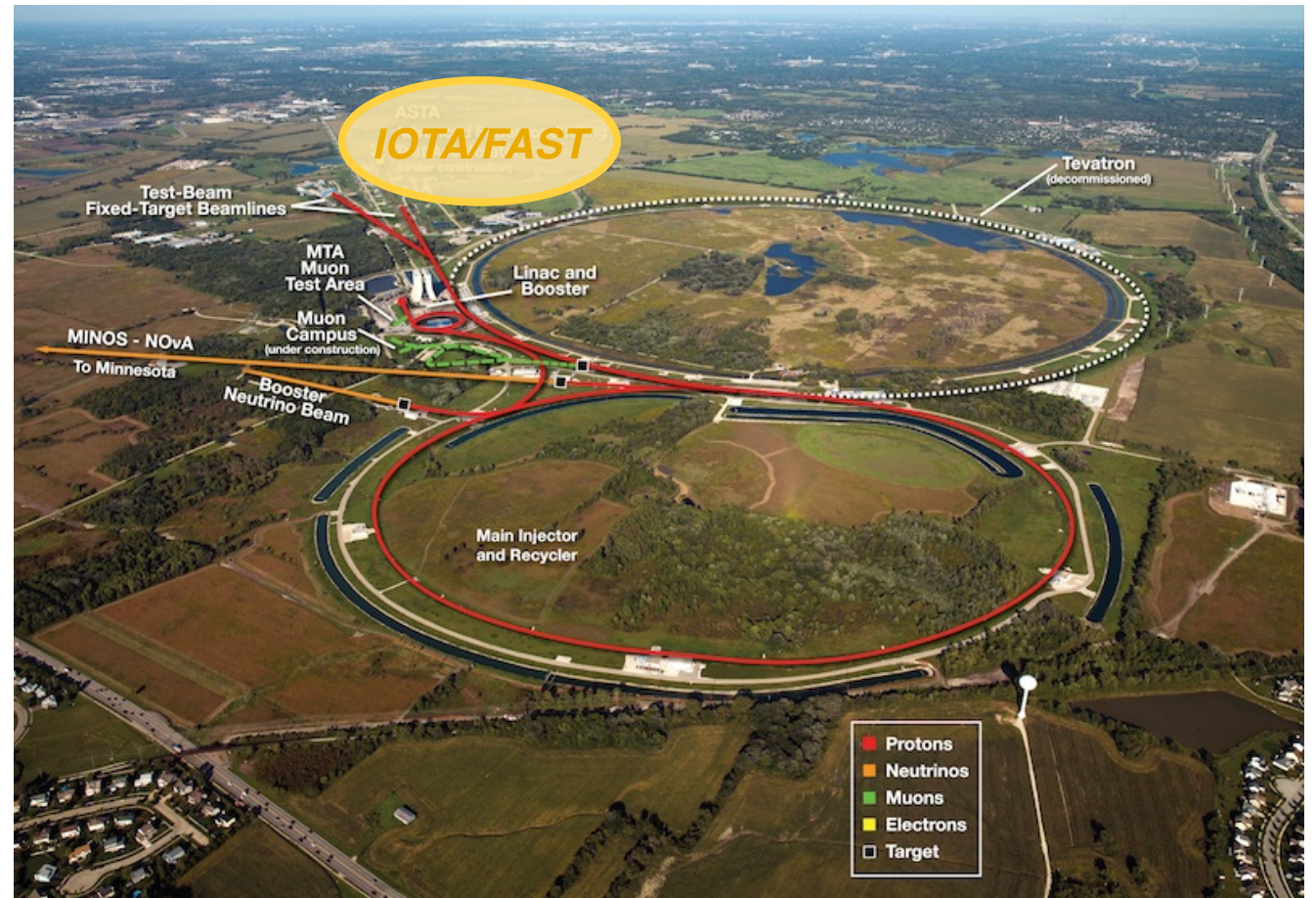
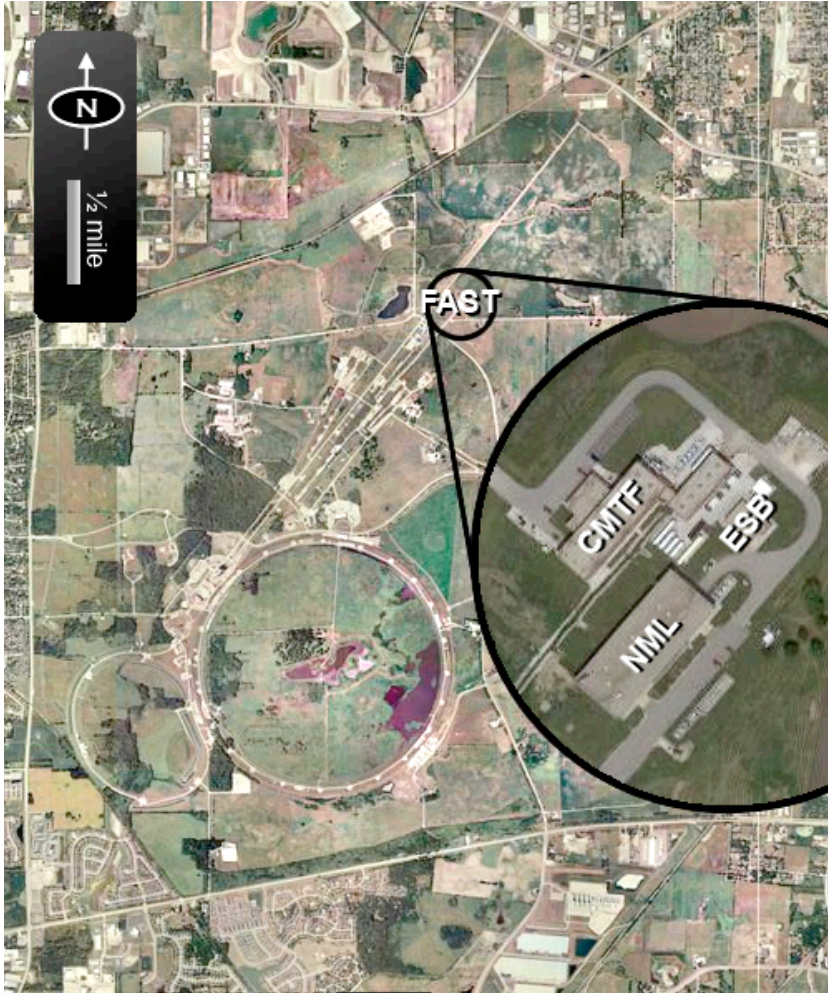


Coincidence rates vs delay: “bunching” and “anti-bunching”

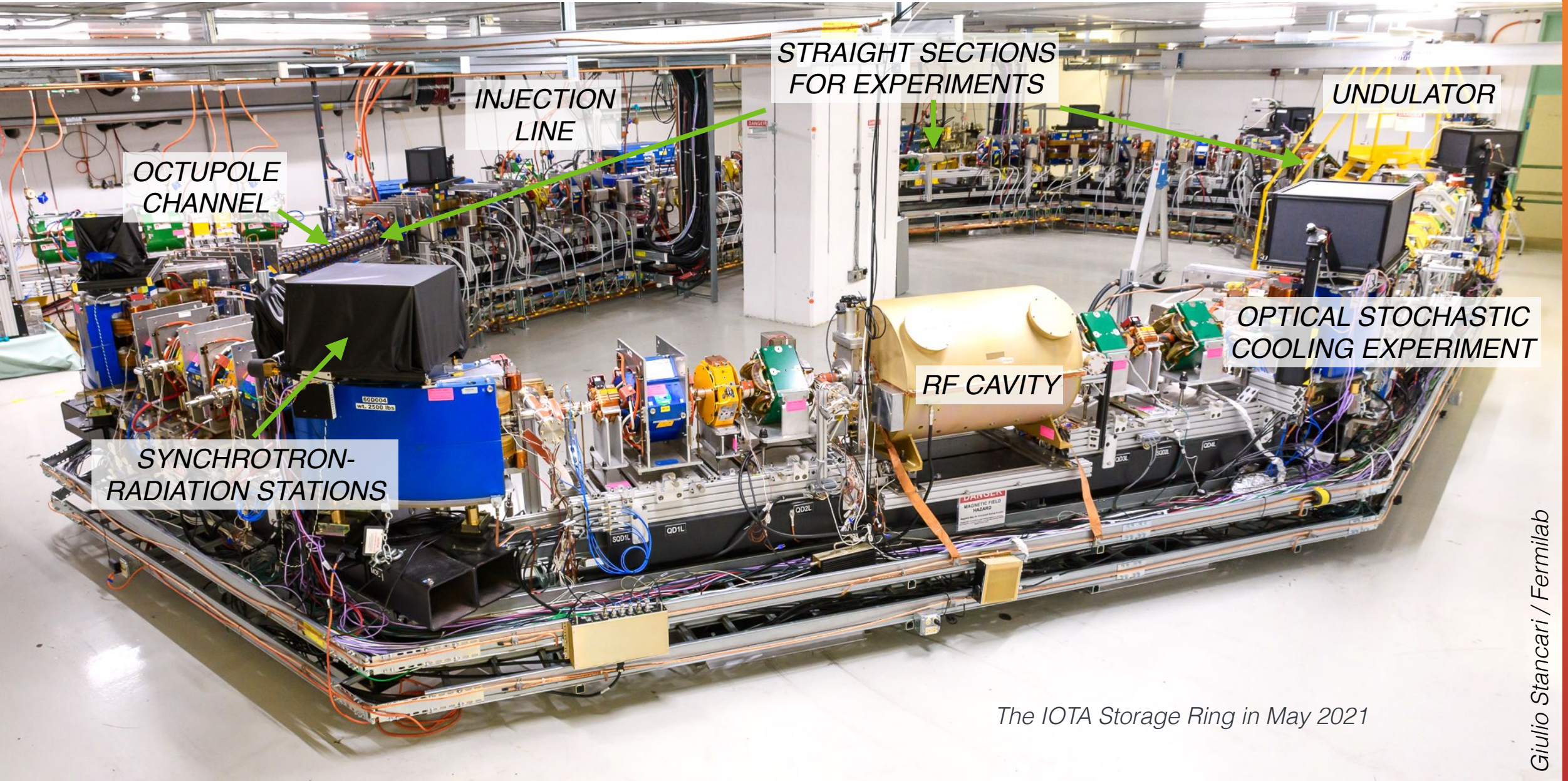
Glauber, Rev. Mod. Phys. **78**, 1267 (2006)

IOTA and the FAST Facility at Fermilab

The Integrable Optics Test Accelerator (IOTA) is part of the Fermilab Accelerator Science and Technology (FAST) facility, located on the north side of the Fermilab campus



The IOTA Storage Ring



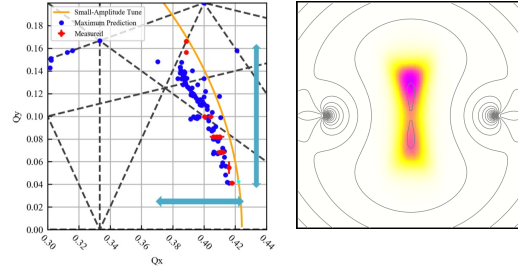
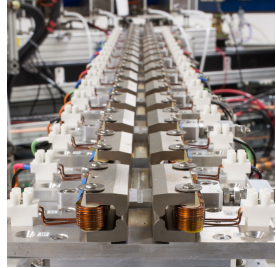
The IOTA Storage Ring in May 2021

Giulio Stancari / Fermilab



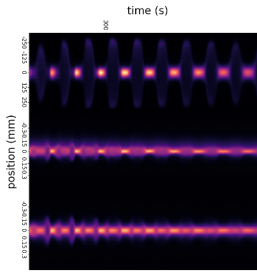
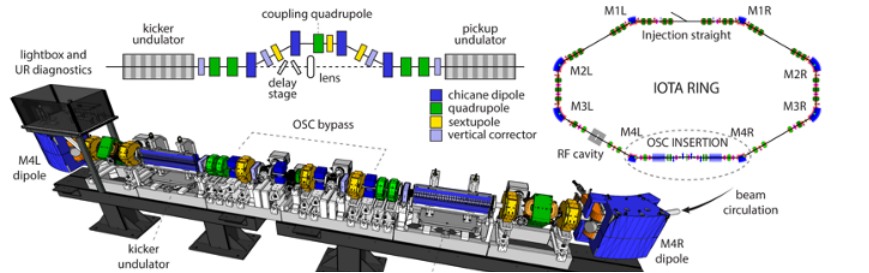
Selected Research Highlights of IOTA Electron Program

Nonlinear Integrable Optics



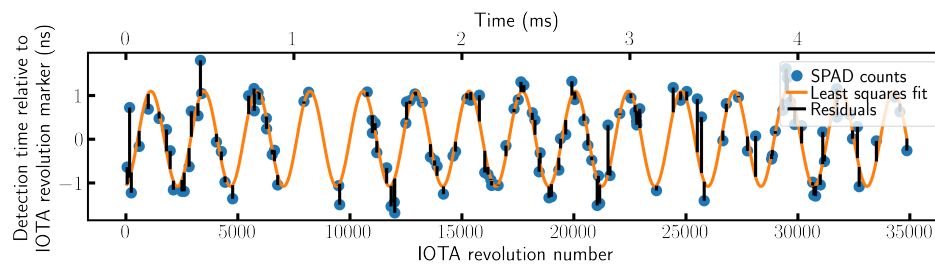
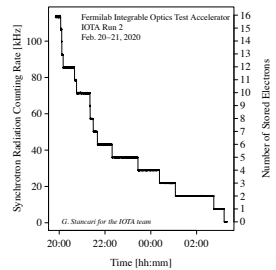
Valishev et al., IPAC 2021
Kuklev, PhD Thesis, U. Chicago (2021)
Szustkowski, PhD Thesis, NIU (2020)
Wieland et al., IPAC 2024
Wieland, PhD Thesis, MSU (2026)

Optical Stochastic Cooling



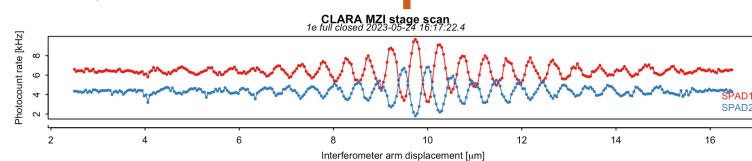
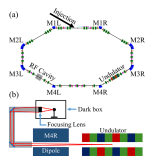
Jarvis, Lebedev, Romanov et al.,
Nature **608**, 287 (2022)

Single-Electron Tracking



Stancari, FERMILAB-FN-1116-AD (2020)
Romanov et al., JINST **16**, P12009 (2021)
Lobach et al., JINST **17**, P02014 (2021)
Romanov et al., IPAC 2024; NAPAC 2025

Classical and Quantum Properties of Radiation

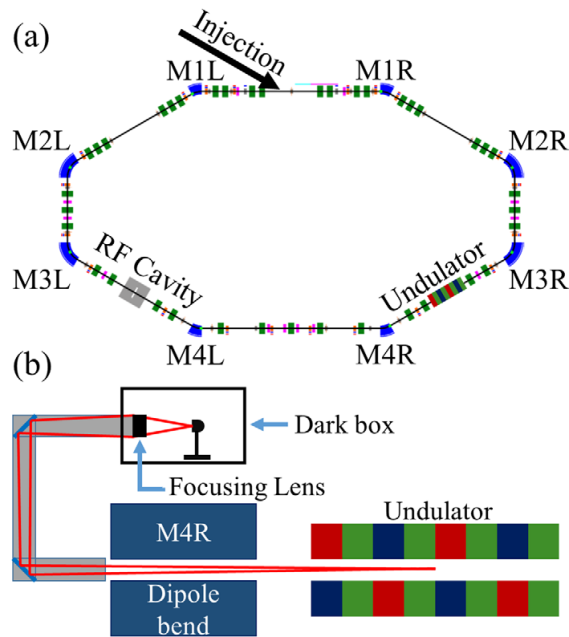


Lobach et al., PRAB **23**, 090703 (2020)
Lobach et al., PRAB **24**, 040701 (2021)
Lobach et al., PRL **126**, 134802 (2021)
Lobach, PhD Thesis (2021)
Stancari et al., IPAC 2024



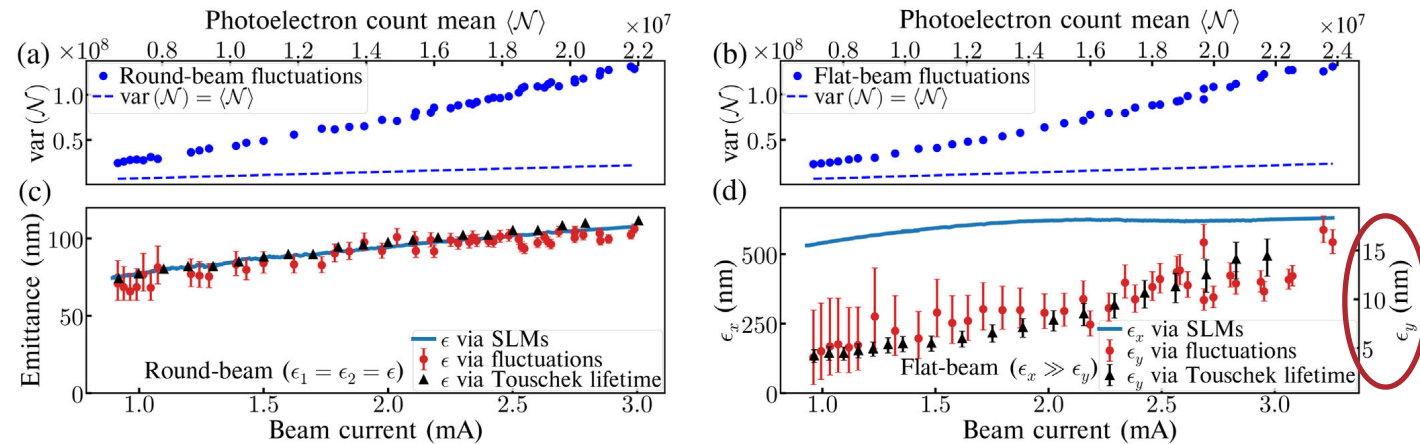
Intensity Fluctuations in Undulator Radiation (FUR)

What are the statistical properties of undulator radiation from single or multiple electrons?
Can they be used for beam diagnostics?

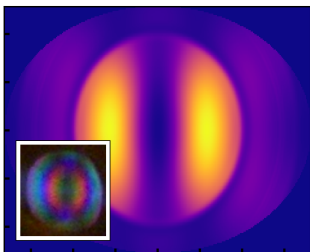


Verified that intensity fluctuations contain a calculable term that depends on beam sizes (interference)

$$\text{var}(\mathcal{N}) = \langle \mathcal{N} \rangle + \frac{\langle \mathcal{N} \rangle^2}{M}$$



Intensity fluctuations can be used to infer small beam emittances



Editors' Suggestion, Featured in Physics

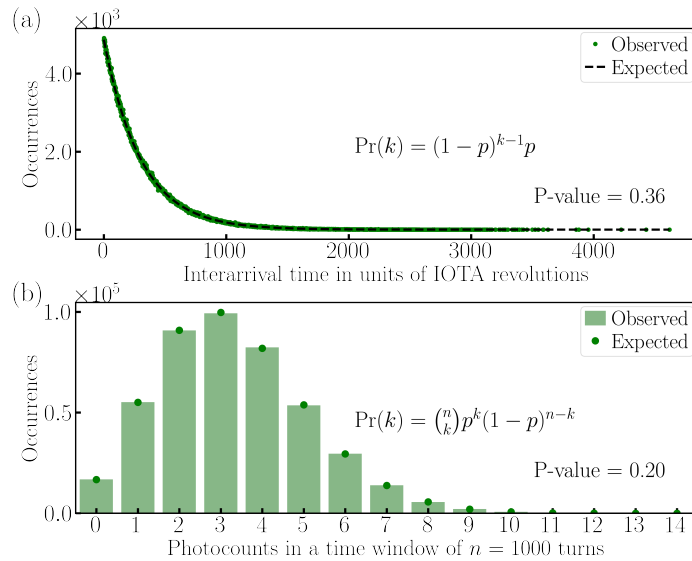
Winner of the 2022 APS DPB Award

- Lobach et al., PRAB **23**, 090703 (2020)
- Lobach et al., PRAB **24**, 040701 (2021)
- Lobach et al., PRL **126**, 134802 (2021)
- Lobach, PhD Thesis (2021)

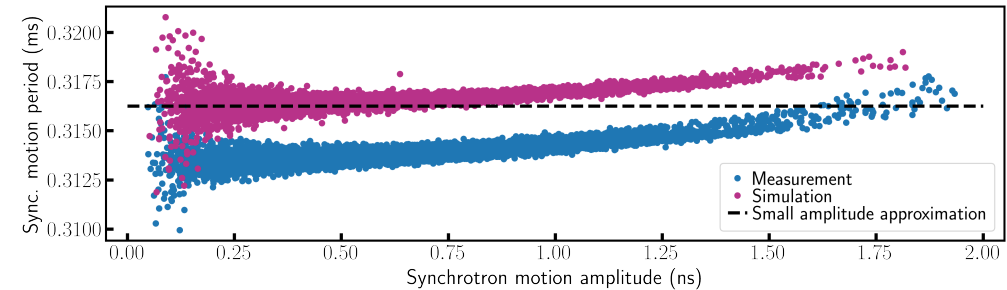


Observations of Photocount Statistics and Timing (URSSE)

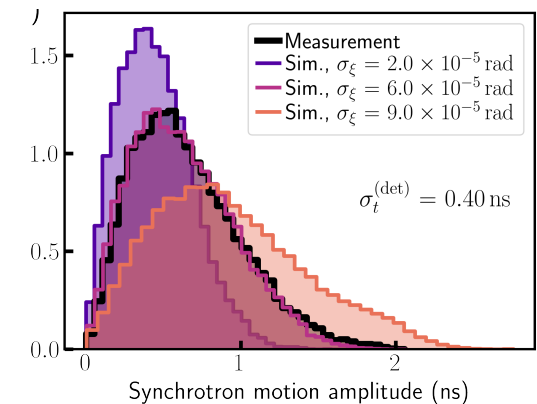
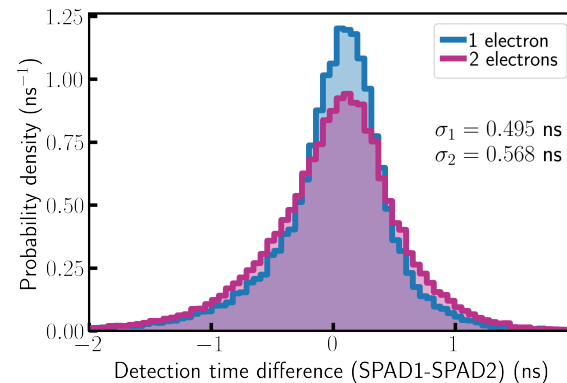
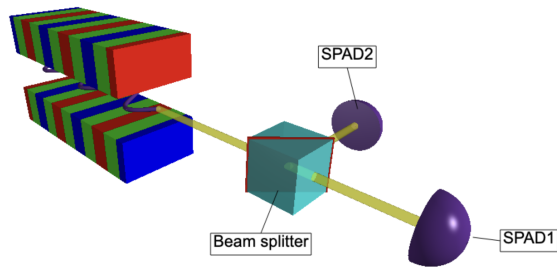
Photocount statistics with a single detector are consistent with a coherent state



From arrival times, measured synchrotron period vs. amplitude and rf phase jitter



Tests with beam splitter and 2 detectors: bunch length vs number of electrons



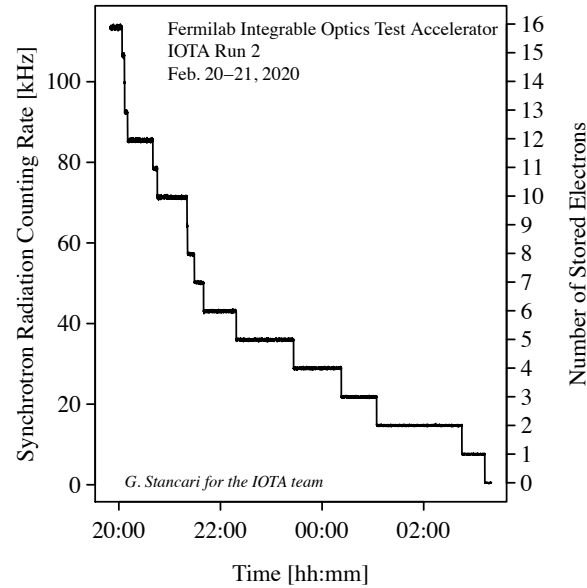
Lobach, PhD Thesis (2021)
Lobach et al., JINST 17, P02014 (2022)



Dynamics of Single Electrons

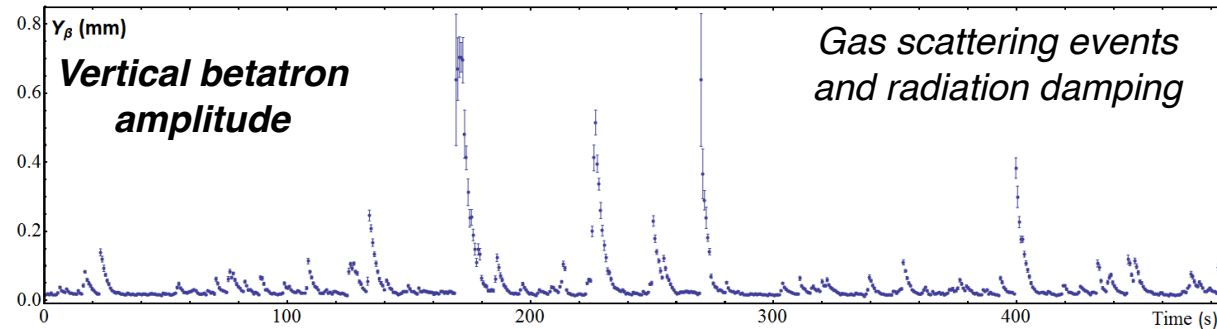
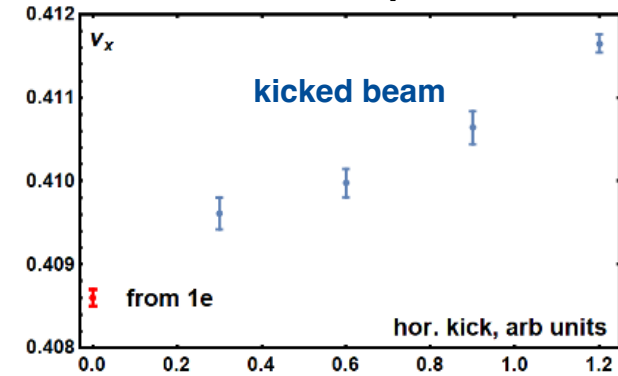
Single electrons (or a known given number of electrons) can be stored for minutes to hours (in a single bucket or multiple buckets)

Discrete steps in intensity decay

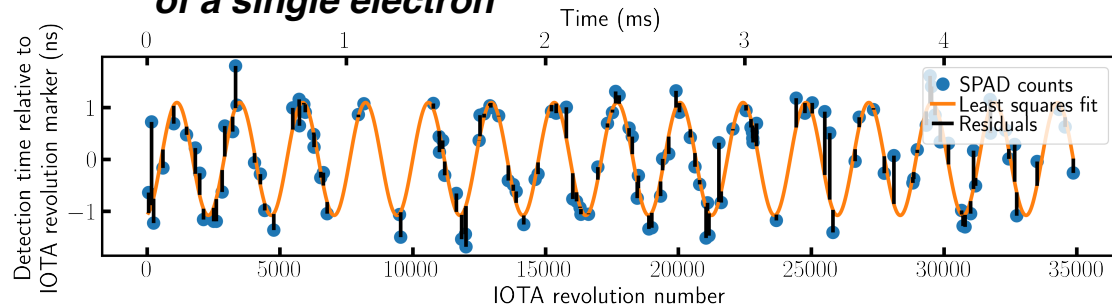


Tracking 1 e^- in all 3 dimensions yields “single particle” lifetimes, emittances, tunes, damping times, beam energies and gas scattering rates

Tune vs. amplitude

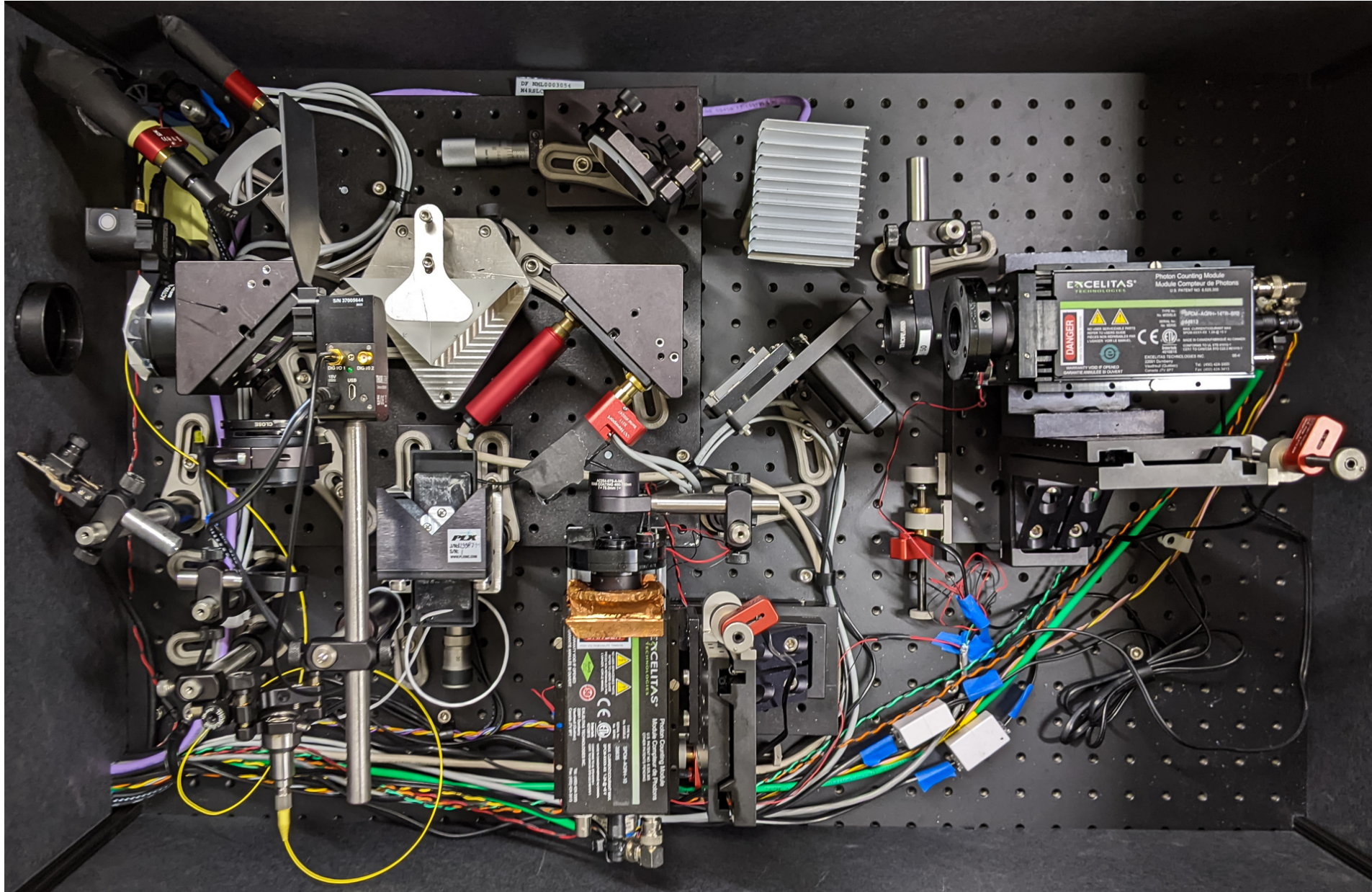


Synchrotron oscillations of a single electron



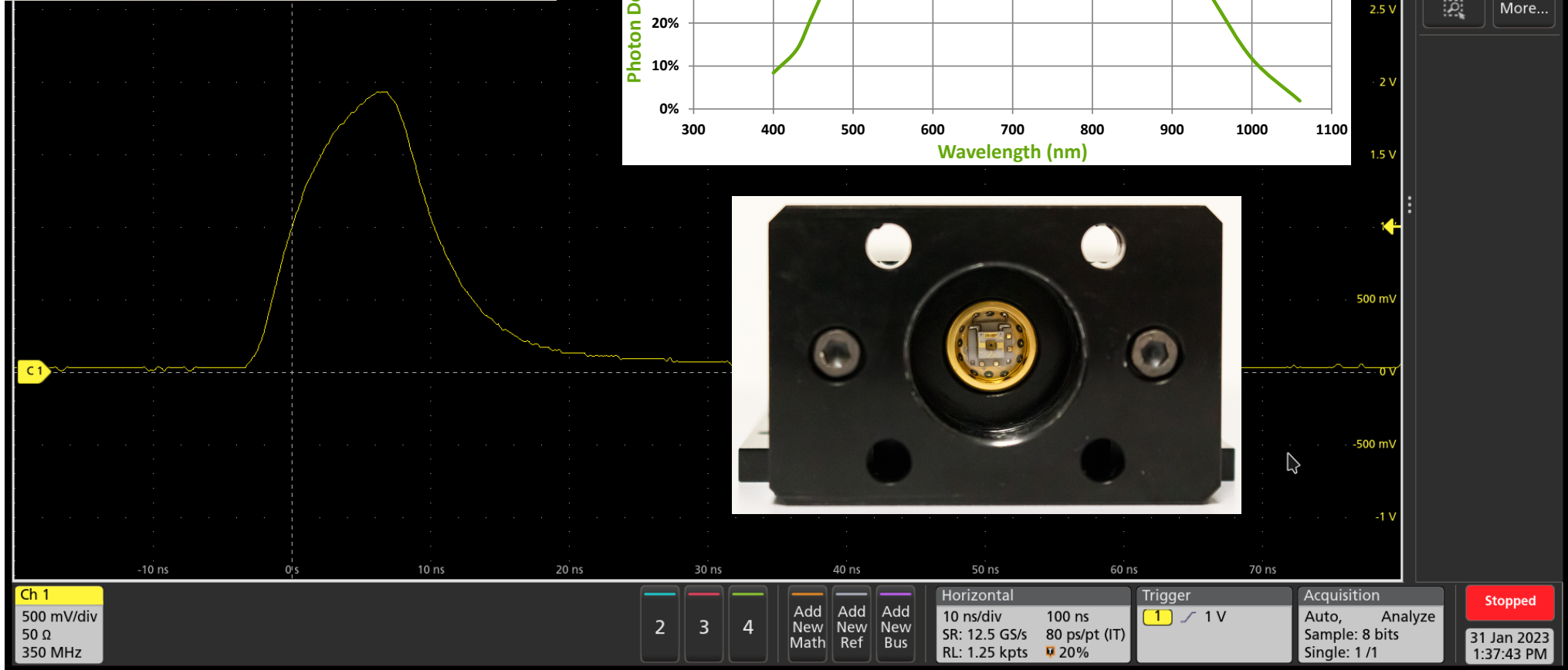
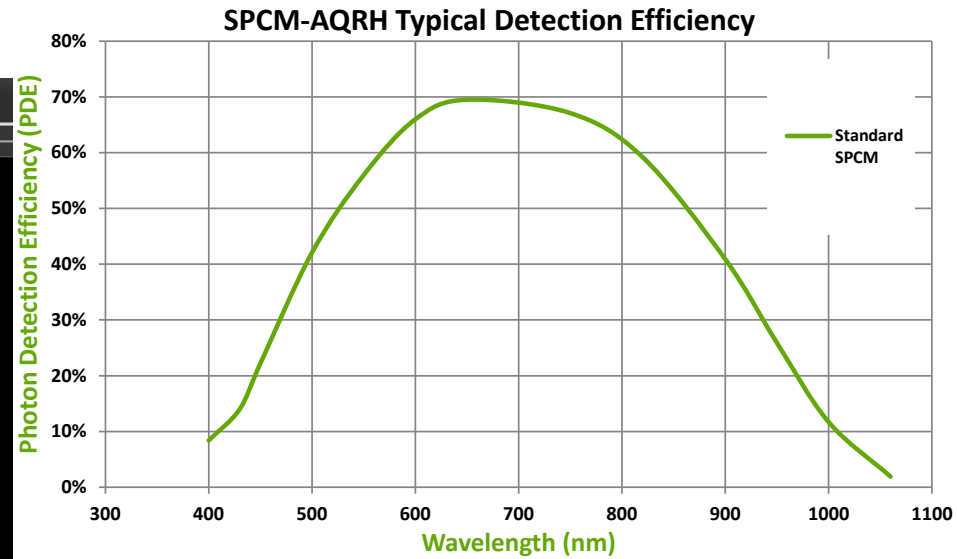
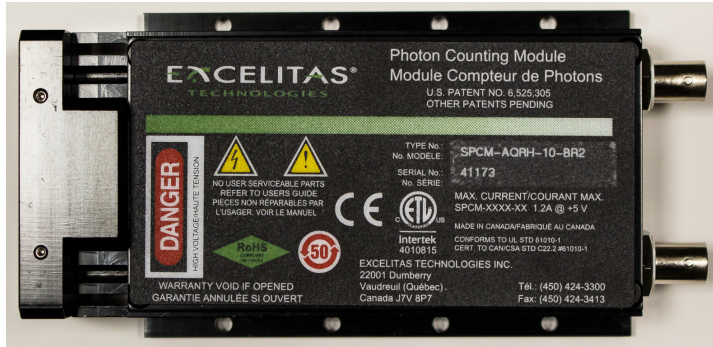
Stancari, FERMILAB-FN-1116-AD (2020)
 Romanov et al., JINST **16**, P12009 (2021)
 Lobach et al., JINST **17**, P02014 (2021)
 Romanov et al., IPAC 2024; NAPAC 2025

The Mach-Zehnder Interferometer (MZI)



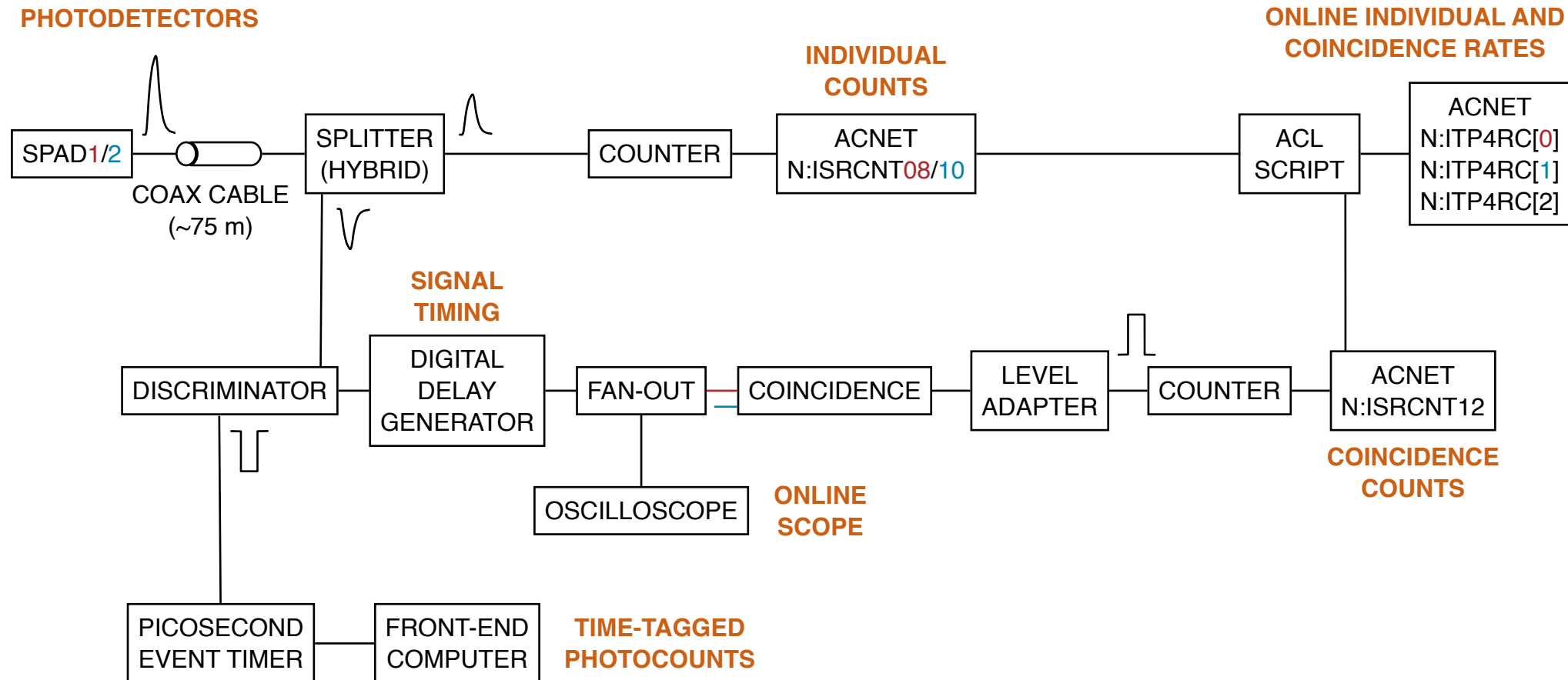


Photodetectors: Single-Photon Avalanche Diodes (SPADs)





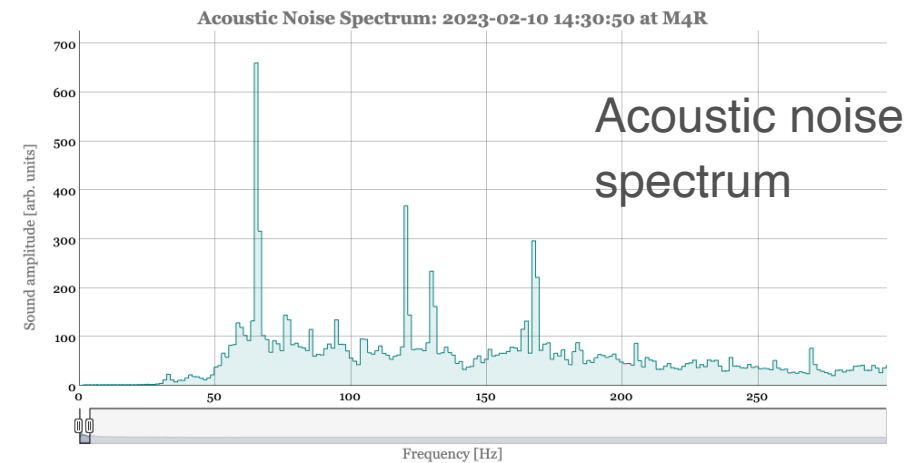
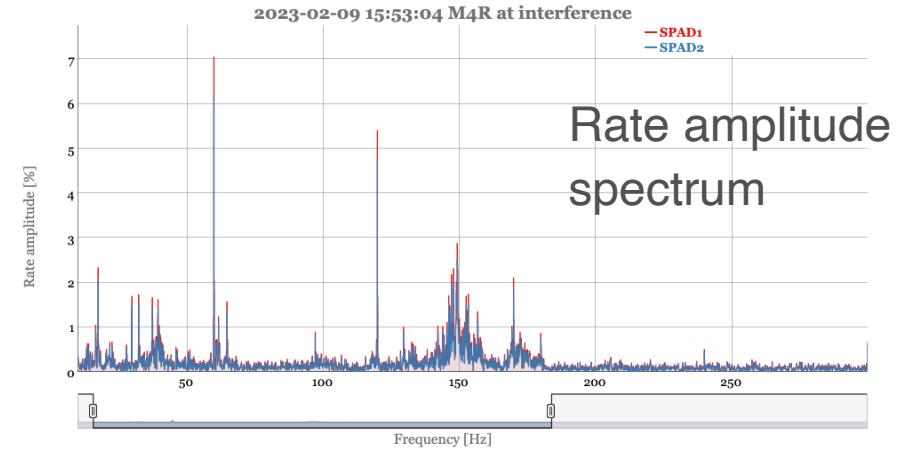
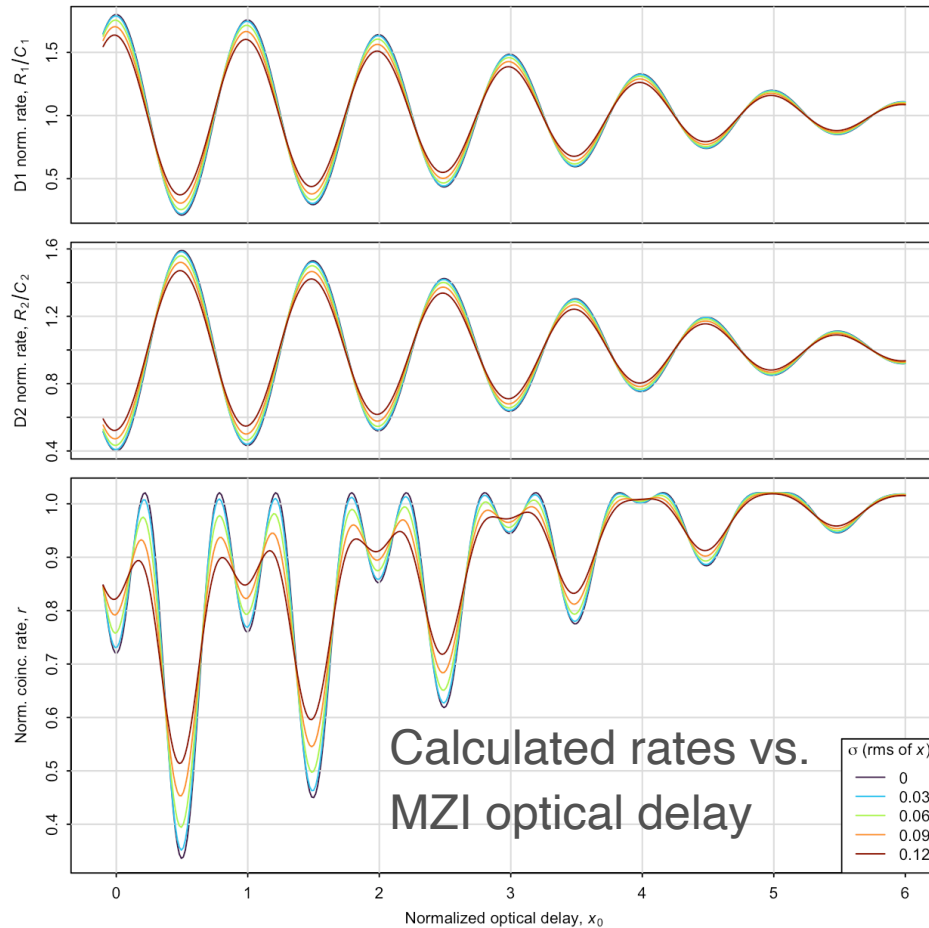
Data Acquisition System



Gated counters, synchronized with the IOTA revolution marker, with similar setup



Mechanical Vibrations Mimic the Hong-Ou-Mandel Effect



Observed mechanical vibrations of 10–20 nm in the ~10–300 Hz range
Apparatus is sensitive to 1% variation in coincidence rate (HOM dip)

Stancari et al., FERMILAB-FN-1246-AD

rpubs.com/gist/clara-vibration-studies DOI:10.5281/zenodo.14897587



Lessons Learned

- Interferometers are of course very sensitive to noise: mechanical vibrations, power-line frequencies, etc.
- Lost detection efficiency at 150 MeV, but could work in parallel with other experiments
- Lengthy alignment procedures of MZI and SPADs; undulator radiation alignment different from laser diode alignment
- If interference condition is lost, it may take a while to re-establish it
- Stage positions need to be synchronized with the rest of the data in control system
- Automatic acquisition of digital camera images could be improved